TECHNICAL REPORT ARCCB-TR-92032

AUTOFRETTAGE--STRESS DISTRIBUTION UNDER LOAD AND RETAINED STRESSES AFTER DEPRESSURIZATION

BOAZ AVITZUR

JULY 1992

US ARMY ARMAMENT RESEARCH,
DEVELOPMENT AND ENGINEERING CENTER
CLOSE COMBAT ARMAMENTS CENTER
BENÉT LABORATORIES
WATERVLIET, N.Y. 12189-4050

APPROVED FOR PUBLIC RELEASE; DISTRIBUTION UNLIMITED

DISCLAIMER

The findings in this report are not to be construed as an official Department of the Army position unless so designated by other authorized documents.

The use of trade name(s) and/or manufacturer(s) does not constitute an official indorsement or approval.

DESTRUCTION NOTICE

For classified documents, follow the procedures in DoD 5200.22-M, Industrial Security Manual, Section II-19 or DoD 5200.1-R, Information Security Program Regulation, Chapter IX.

For unclassified, limited documents, destroy by any method that will prevent disclosure of contents or reconstruction of the document.

For unclassified, unlimited documents, destroy when the report is no longer needed. Do not return it to the originator.

REPORT DOCUMENTATION PAGE

Form Approved
OMB No. 0704-0188

1. AGENCY USE ONLY (Leave blank)	2. REPORT DATE	3. REPORT TYPE AND DATES COVERED
	July 1992	Final

4. TITLE AND SUBTITLE

AUTOFRETTAGE--STRESS DISTRIBUTION UNDER LOAD AND RETAINED STRESSES AFTER DEPRESSURIZATION

5. FUNDING NUMBERS

AMCMS No. 6436.39.6430.012
PRON No. 4A7HF7YF/F1A

6. AUTHOR(S)

Boaz Avitzur

7. PERFORMING ORGANIZATION NAME(S) AND ADDRESS(ES)

U.S. Army ARDEC
Benet Laboratories, SMCAR-CCB-TL
Watervliet, NY 12189-4050

8. PERFORMING ORGANIZATION REPORT NUMBER

ARCCB-TR-92032

9. SPONSORING / MONITORING AGENCY NAME(S) AND ADDRESS(ES)

U.S. Army ARDEC
Close Combat Armaments Center
Picatinny Arsenal, NJ 07806-5000

10. SPONSORING / MONITORING AGENCY REPORT NUMBER

11. SUPPLEMENTARY NOTES

This report supersedes ARDEC Technical Report ARCCB-TR-89019 dated July 1989.

12a. DISTRIBUTION / AVAILABILITY STATEMENT

Approved for public release; distribution unlimited.

12b. DISTRIBUTION CODE

13. ABSTRACT *(Maximum 200 words)*

There is a long-standing interest in developing a capability to predict the distribution of retained stresses in thick-walled tubes after the removal of an internal pressure--post autofrettage. In this report, four different methods of calculating such stresses are presented and compared. The methods presented are based on the following assumed yield criteria and deformation conditions:

1. Tresca's yield criterion
2. Tresca's yield criterion times $2/\sqrt{3}$
3. Mises' yield criterion in plane-stress
4. Mises' yield criterion in plane-strain

14. SUBJECT TERMS

Autofrettage, Thick-Walled Tubes, Stress Distribution, Retained Stresses, Tresca's Yield Criterion, Mises' Yield Criterion, Plane-Stress, Plane-Strain

15. NUMBER OF PAGES
39

16. PRICE CODE

17. SECURITY CLASSIFICATION OF REPORT	18. SECURITY CLASSIFICATION OF THIS PAGE	19. SECURITY CLASSIFICATION OF ABSTRACT	20. LIMITATION OF ABSTRACT
UNCLASSIFIED	UNCLASSIFIED	UNCLASSIFIED	UL

TABLE OF CONTENTS

LIST OF ILLUSTRATIONS

A-1

NOMENCLATURE

a ≡ tube's bore radius

b ≡ tube's outer radius

E ≡ material's modulus of elasticity

p ≡ pressure

p_i ≡ internal pressure at the tube's bore

p_o ≡ external pressure at the tube's outer diameter

r ≡ radial distance

u ≡ displacement

z ≡ coordinate's direction in a cartesian coordinate system

δ ≡ $1 - \nu + \nu^2$

ϵ ≡ strain

η ≡ $(1-2\nu)^2$

ν ≡ material's Poisson's factor

σ ≡ stress

σ_o ≡ material's yield strength

ρ ≡ radius of elastic-plastic interface

Subscripts

i ≡ at the tube's inner diameter

o ≡ at the tube's outer diameter

r ≡ a coordinate's plane and/or a coordinate's direction in a cylindrical coordinate system

z ≡ a coordinate's plane and/or a coordinate's direction in a cylindrical coordinate system

θ ≡ a coordinate's plane and/or a coordinate's direction in a cylindrical coordinate system

( ) ≡ a subscript inside parentheses indicates a specific geometrical location, i.e., $\sigma_{rr(a)} = \sigma_{rr}$ @ $r = a$ or $\sigma_{\theta\theta(c)} = \sigma_{\theta\theta}$ @ $r = c$

INTRODUCTION

Autofrettage is a process in which a thick-walled tube is pressurized internally beyond its elastic limit. Reaching the elastic limit initiates plastic flow at the tube's bore (inner surface, r=a). Gradual increases of the pressure at the bore are accompanied by a progressive thickening of the plastically deformed inner sleeve. This plastically deformed sleeve is in the range $a \leq r \leq \rho$, with the elastic-plastic interface at $r=\rho$ (where $a \leq \rho \leq b$). This process is commonly used in the manufacturing of some thick-walled pressure vessels. Its application as a manufacturing process generated an interest in correlating the imposed pressure (usually an internal one) with the elastic-plastic interface at $r=\rho$, and with the distribution of the retained state of stress throughout the wall thickness upon the removal of that pressure.

The elastic stress distribution in plane-stress in an axisymmetrically loaded thick-walled tube, according to Timoshenko and Goodier (ref 1), is shown in Eqs. (1a) and (1b) (otherwise known as the Lamé solution).

$$\sigma_{\theta\theta(r)} = - \frac{[(\frac{b}{a})^2 + (\frac{b}{r})^2]p_o - [(\frac{b}{r})^2 + 1]p_i}{(\frac{b}{a})^2 - 1} \qquad (1a)$$

and

$$\sigma_{rr(r)} = - \frac{[(\frac{b}{a})^2 - (\frac{b}{r})^2]p_o + [(\frac{b}{r})^2 - 1]p_i}{(\frac{b}{a})^2 - 1} \qquad (1b)$$

where p_i = an internal pressure and p_o = an external pressure. These equations satisfy the Airy stress function (ref 2), as required, throughout the elastic

[1] S. Timoshenko and J. N. Goodier, Theory of Elasticity, Second Edition, Engineering Societies Monographs, 1951.
[2] A. E. H. Love, A Treatise of the Mathematical Theory of Elasticity, Fourth Edition, Dover Publications, New York, 1944, pp. 102-103.

wall thickness of the tube, provided $\sigma_{rr(i)} \equiv -p_i$ and $\sigma_{rr(o)} \equiv -p_o$ are applied at radiuses $r = r_i$ and $r = r_o$, respectively. These can be either within the elastic region or at its boundaries.

It can be shown that if either of the boundaries, r=a or r=b, is replaced by an inner surface at r=d (where $a \leq d \leq b$) and the radial stress, $\sigma_{rr(d)}$ (at r=d), that prevails under the above imposed external pressure at that surface is assigned to it (as if it were an external pressure on an external surface at r=d), then the Lamé equations describe the stress distribution in the remaining elastic sleeve. That is,

$$\sigma_{\theta\theta(r)} = - \frac{[(\frac{b}{d})^2 + (\frac{b}{r})^2]p_o + [(\frac{b}{r})^2 + 1]\sigma_{rr(d)}}{(\frac{b}{d})^2 - 1} \qquad (1'a)$$

$$\sigma_{rr(r)} = - \frac{[(\frac{b}{d})^2 - (\frac{b}{r})^2]p_o - [(\frac{b}{r})^2 - 1]\sigma_{rr(d)}}{(\frac{b}{d})^2 - 1} \qquad (1'b)$$

for the range $d \leq r \leq b$, or

$$\sigma_{\theta\theta(r)} = \frac{[(\frac{d}{a})^2 + (\frac{d}{r})^2]\sigma_{rr(d)} - [(\frac{d}{r})^2 + 1]p_i}{(\frac{d}{a})^2 - 1} \qquad (1''a)$$

$$\sigma_{rr(r)} = \frac{[(\frac{d}{a})^2 - (\frac{d}{r})^2]\sigma_{rr(d)} + [(\frac{d}{r})^2 - 1]p_i}{(\frac{d}{a})^2 - 1} \qquad (1''b)$$

for the range $a \leq r \leq d$. Thus, if the surface $r=\rho$ (where $a \leq \rho \leq b$) is the elastic-plastic interface, then the stress at that surface satisfies the Lamé equations (1'a) and (1'b) and the selected yield criterion simultaneously.

After determining the radial stress, $\sigma_{rr(\rho)}$, at the elastic-plastic interface and knowing the external pressure, p_o, at the tube's external surface at r=b, one can use Eqs. (1'a) and (1'b) (with d being replaced by ρ) to determine the stress distribution in the tube's elastic region, $\rho \leq r \leq b$.

In the absence of such equations as Hooke's Law for the plastically deformed material (while certain continuities in strain and stress have to be satisfied), exact solutions for such problems are, in general, difficult to obtain (ref 3). However, in problems such as beam bending and autofrettage where the plastic deformation is constrained by the elastic portion of the subject body, some solutions can be offered. The key to a solution for the stress distribution in the plastic region of an autofrettaged tube is the stress equilibrium. As shown by Manning (ref 4) and as demonstrated in Figure 1 of this report, equilibrium in the r-θ plane is satisfied when

$$\frac{d\sigma_{rr}}{\sigma_{\theta\theta} - \sigma_{rr}} = \frac{dr}{r} \tag{2}$$

It can be shown that the Lamé equations satisfy Eq. (2) and thus equilibrium prevails throughout the elastic region. Furthermore, if one expresses $\sigma_{\theta\theta} - \sigma_{rr}$ in terms that explicitly satisfy a given yield criterion, then the solution to Eq. (2), with that condition at r=ρ as a boundary condition, describes the stress field in the plastic region, $a \leq r \leq \rho$.

MISES' YIELD CRITERION IN PLANE-STRESS

Mises' yield criterion assumes that when

$$\sqrt{\tfrac{1}{2}[(\sigma_{\theta\theta}-\sigma_{rr})^2 + (\sigma_{rr}-\sigma_{zz})^2 + (\sigma_{\theta\theta}-\sigma_{zz})^2]} = \sigma_o \tag{3}$$

[3]Betzalel Avitzur, Metal Forming: Processes and Analysis, McGraw-Hill Book Company, 1968, Chapters 4 and 5.
[4]W. R. D. Manning, "The Overstrain of Tubes by Internal Pressure," Engineering, Vol. 159, 1945, pp. 101-102 and 183-184.

yielding takes place. In plane-stress, where $\sigma_{zz} = 0$, Eq. (3) reduces to

$$\sqrt{\sigma_{\theta\theta}^2 + \sigma_{rr}^2 - \sigma_{\theta\theta} \cdot \sigma_{rr}} = \sigma_o \qquad (4)$$

According to the Lamé solution for the elastic region

$$\sigma_{\theta\theta(\rho)} = \frac{-2(\frac{b}{\rho})^2 \cdot p_o - [(\frac{b}{\rho})^2 + 1]\sigma_{rr(\rho)}}{(\frac{b}{\rho})^2 - 1} \qquad (5)$$

Thus, at the elastic-plastic interface, $r=\rho$, Eq. (4) becomes

$$\frac{\{2(\frac{b}{\rho})^2 \cdot p_o + [(\frac{b}{\rho})^2 + 1]\sigma_{rr(\rho)}\}^2}{[(\frac{b}{\rho})^2 - 1]^2} + \sigma_{rr(\rho)}^2$$

$$+ \frac{2(\frac{b}{\rho})^2 p_o + [(\frac{b}{\rho})^2 + 1]\sigma_{rr(\rho)}}{(\frac{b}{\rho})^2 - 1} \cdot \sigma_{rr(\rho)} = \sigma_o^2$$

or

$$\{[(\frac{b}{\rho})^2 + 1]^2 + [(\frac{b}{\rho})^2 - 1]^2 + [(\frac{b}{\rho})^4 - 1]\}\sigma_{rr(\rho)}^2 + \{4[(\frac{b}{\rho})^2 + 1]$$

$$+ 2[(\frac{b}{\rho})^2 - 1]\}(\frac{b}{\rho})^2 \cdot p_o \cdot \sigma_{rr(\rho)} + 4(\frac{b}{\rho})^4 \cdot p_o^2 - [(\frac{b}{\rho})^2 - 1]^2\sigma_o^2 = 0$$

or

$$[3(\frac{b}{\rho})^4 + 1]\sigma_{rr(\rho)}^2 - 2[3(\frac{b}{\rho})^2 + 1](\frac{b}{\rho})^2 \cdot p_o \cdot \sigma_{rr(\rho)} + 4(\frac{b}{\rho})^4 p_o^2$$

$$- [(\frac{b}{\rho})^2 - 1]^2\sigma_o^2 = 0$$

Thus,

$$\sigma_{rr(\rho)} = \frac{[3(\frac{b}{\rho})^2+1](\frac{b}{\rho})^2 \cdot p_o \pm \sqrt{[3(\frac{b}{\rho})^2+1]^2(\frac{b}{\rho})^4 \cdot p_o^2 - [3(\frac{b}{\rho})^4+1]\{4(\frac{b}{\rho})^4 p_o^2 - [(\frac{b}{\rho})^2-1]^2 \sigma_o^2\}}}{3(\frac{b}{\rho})^4 + 1}$$

or

$$\sigma_{rr(\rho)} = \frac{[3(\frac{b}{\rho})^2+1](\frac{b}{\rho})^2 \cdot p_o \pm \sqrt{[(\frac{b}{\rho})^2-1]^2\{[3(\frac{b}{\rho})^4+1]\sigma_o^2 - 3(\frac{b}{\rho})^4 \cdot p_o^2\}}}{3(\frac{b}{\rho})^4 + 1}$$

from which

$$\sigma_{rr(\rho)} = \frac{[3(\frac{b}{\rho})^2+1](\frac{b}{\rho})^2 p_o \pm [(\frac{b}{\rho})^2 - 1]\sqrt{[3(\frac{b}{\rho})^4+1]\sigma_o^2 - 3(\frac{b}{\rho})^4 p_o^2}}{3(\frac{b}{\rho})^4 + 1} \qquad (6)$$

For $p_o = 0$ and due to internal pressurization, Eq. (6) is reduced to

$$\sigma_{rr(\rho)} = -\frac{(\frac{b}{\rho})^2 - 1}{\sqrt{3(\frac{b}{\rho})^4 + 1}} \cdot \sigma_o \qquad (7)$$

With the radial stresses known at the boundaries of the elastic region, $\sigma_{rr(b)} = -p_o$ at the tube's outer surface, r=b, and $\sigma_{rr(\rho)}$ as expressed by Eq. (6) (or Eq. (7) in the absence of pressure at the tube's outer diameter (OD)), the stress distribution throughout the elastic range is determined by Eqs. (1'a) and (1'b), where $d = \rho$. For the case of $p_o = 0$, one gets

$$\sigma_{\theta\theta(r)} = \frac{(\frac{b}{r})^2 + 1}{\sqrt{3(\frac{b}{\rho})^4 + 1}} \cdot \sigma_o \qquad (8a)$$

and

$$\sigma_{rr(r)} = -\frac{\left(\frac{b}{r}\right)^2 - 1}{\sqrt{3\left(\frac{b}{\rho}\right)^4 + 1}} \cdot \sigma_o \qquad (8b)$$

From Eq. (4) one gets

$$\sigma_{\theta\theta} = \frac{\sigma_{rr} \pm \sqrt{4\sigma_o^2 - 3\sigma_{rr}^2}}{2} \qquad (9)$$

and thus

$$\sigma_{\theta\theta} - \sigma_{rr} = \frac{-\sigma_{rr} \pm \sqrt{4\sigma_o^2 - 3\sigma_{rr}^2}}{2}$$

Hence, for the case of internal pressurization, where $\sigma_{rr} < 0$ and $\sigma_{\theta\theta} > 0$, Eq. (2) reads

$$\frac{d\sigma_{rr}}{\sigma_{rr} + \sqrt{4\sigma_o^2 - 3\sigma_{rr}^2}} = -\frac{1}{2} \cdot \frac{dr}{r} \qquad (10)$$

and the solution to Eq. (10), with Eq. (8b) as its boundary condition, is (ref 5)

$$\ln \frac{r}{\rho} = -\frac{1}{4}\left\{\ln \frac{\left[\sqrt{3} \cdot \sqrt{\frac{4}{3}\left(\frac{\sigma_o}{\sigma_{rr(r)}}\right)^2 - 1} + 1\right]^2}{4\left(\frac{\sigma_o}{\sigma_{rr(r)}}\right)^2} - \ln \frac{4\left(\frac{b}{\rho}\right)^4}{3\left(\frac{b}{\rho}\right)^4 - 1}\right. \qquad (11)$$

$$\left. -2 \cdot \sqrt{3}\left[\tan^{-1}\sqrt{\frac{4}{3}\left(\frac{\sigma_o}{\sigma_{rr(r)}}\right)^2 - 1} - \tan^{-1}\frac{3\left(\frac{b}{\rho}\right)^2 + 1}{\sqrt{3}\left[\left(\frac{b}{\rho}\right)^2 - 1\right]}\right]\right\}$$

Equation (11) yields an explicit relation between the surface at r and the radial stress, $\sigma_{rr(r)}$, on it. Having $\sigma_{rr(r)}$ determined and with the aid of Eq. (9), which for the case of internal pressurization assumes the form

[5] R. Weigle, "Elastic-Plastic Analysis of a Cylindrical Tube," WVT-RR-6007, Watervliet Arsenal, Watervliet, NY, March 1960.

$$\sigma_{\theta\theta} = \frac{\sigma_{rr} - \sqrt{4\sigma_o^2 - 3\sigma_{rr}^2}}{2} \qquad (9')$$

one can compute the corresponding tangential (hoop) stress, $\sigma_{\theta\theta(r)}$, at any surface r, within the plastic region, $a \leq r \leq \rho$.

MISES' YIELD CRITERION IN PLANE-STRAIN

The Lamé equations, which have been derived for the stress distribution in the elastic region, are two-dimensional in nature and thus apply to plane-stress problems. However, their resultant axial strain, ϵ_{zz}, as shown by Eq. (12), is uniform throughout the elastic region, $\rho \leq r \leq b$.

$$\epsilon_{zz} = \frac{\nu}{E}(\sigma_{rr} + \sigma_{\theta\theta}) = -\frac{2\nu}{E} \cdot \frac{(\frac{b}{\rho})^2 \cdot p_o - \sigma_{rr(\rho)}}{(\frac{b}{\rho})^2 - 1} \qquad (12)$$

Therefore, if a physical constraint of $\epsilon_{zz} = 0$ is imposed, the axial stress distribution, σ_{zz}, throughout the elastic region is uniform. Thus, it is assumed that Lamé's relation of the tangential (hoop) and the radial stresses to the stresses at the boundaries also prevails in the plane-strain condition. In conjunction with these stresses, a uniform axial stress of

$$\sigma_{zz} = -2\nu \cdot \frac{(\frac{b}{\rho})^2 \cdot p_o - \sigma_{rr(\rho)}}{(\frac{b}{\rho})^2 - 1} \qquad (13)$$

exists.

Thus, at the elastic-plastic interface, $r=\rho$, where yielding commences, Mises' criterion can be reduced to

$$\sqrt{(1-\nu+\nu^2)\sigma_{\theta\theta}^2 - (1+2\nu-2\nu^2)\sigma_{\theta\theta} \cdot \sigma_{rr} + (1-\nu+\nu^2) \cdot \sigma_{rr}^2} = \sigma_o \qquad (14)$$

from which

$$\sigma_{\theta\theta} = \frac{(1+2\nu-2\nu^2)\sigma_{rr} \pm \sqrt{4(1-\nu+\nu^2)\sigma_o^2 - 3(1-2\nu)^2\sigma_{rr}^2}}{2(1-\nu+\nu^2)} \tag{15}$$

By applying the values of $\sigma_{\theta\theta}$ and σ_{rr} from the Lamé solution (Eqs. (1'a) and (1'b)) at the elastic-plastic interface to Eq. (14), one gets

$$\sigma_{rr(\rho)} = \frac{[3(\frac{b}{\rho})^2+(1-2\nu)^2](\frac{b}{\rho})^2 \cdot p_o \pm [(\frac{b}{\rho})^2-1] \cdot \sqrt{[3(\frac{b}{\rho})^4+(1-2\nu)^2]\sigma_o^2-3(1-2\nu)^2(\frac{b}{\rho})^2 \cdot p_o^2}}{3(\frac{b}{\rho})^4 + (1-2\nu)^2} \tag{16}$$

which for an internally pressurized tube with no external pressure, $p_o = 0$, is reduced to

$$\sigma_{rr(\rho)} = -\frac{(\frac{b}{\rho})^2 - 1}{\sqrt{3(\frac{b}{\rho})^4 + (1-2\nu)^2}} \cdot \sigma_o \tag{17}$$

By applying Eq. (17) to Eqs. (1'a) and (1'b), one gets Eqs. (18a) and (18b), respectively. This procedure is similar to the one used in deriving Eqs. (8a) and (8b) and in the absence of external pressure, $p_o = 0$ (at the tube's outer surface, r=b), one gets the following for the stress distribution in the elastic region, $\rho \leq r \leq b$, of the tube:

$$\sigma_{\theta\theta(r)} = \frac{(\frac{b}{r})^2 + 1}{\sqrt{3(\frac{b}{\rho})^4 + (1-2\nu)^2}} \cdot \sigma_o \tag{18a}$$

$$\sigma_{rr(r)} = -\frac{(\frac{b}{r})^2 - 1}{\sqrt{3(\frac{b}{\rho})^4 + (1-2\nu)^2}} \cdot \sigma_o \tag{18b}$$

Since the plastic strain is the same order of magnitude as the elastic strain, it is assumed that in the case of plane-strain, the axial stress in the plastic region complies with Hooke's Law (as expressed in Eq. (13)). Thus, Eq. (15) yields

$$\sigma_{\theta\theta} - \sigma_{rr} = - \frac{(1-2\nu)^2 \cdot \sigma_{rr} + \sqrt{4(1-\nu+\nu^2)\sigma_o^2 - 3(1-2\nu)^2\sigma_{rr}^2}}{2(1-\nu+\nu^2)}$$

and equilibrium prevails when

$$\frac{d\sigma_{rr}}{(1-2\nu)^2\sigma_{rr} + \sqrt{4(1-\nu+\nu^2)\sigma_o^2 - 3(1-2\nu)^2\sigma_{rr}^2}} = - \frac{1}{2(1-\nu+\nu^2)} \cdot \frac{dr}{r} \qquad (19)$$

The solution of which with Eq. (17) as its boundary condition, is

$$\ln \frac{r}{\rho} = \frac{1}{4} \left\{ \ln \frac{\left[\sqrt{\frac{3}{\eta}} \cdot \sqrt{\frac{4}{3}\frac{\delta}{\eta}\left(\frac{\sigma_o}{\sigma_{rr(r)}}\right)^2 - 1} + 1\right]^2}{4\frac{\delta}{\eta^2}\left(\frac{\sigma_o}{\sigma_{rr(r)}}\right)^2} - \ln \frac{(3+\eta)\left(\frac{b}{\rho}\right)^4}{3\left(\frac{b}{\rho}\right)^4 + \eta} \right.$$

$$\left. -2\sqrt{\frac{3}{\eta}} \cdot \left[\tan^{-1}\sqrt{\frac{4\delta}{3\eta}\left(\frac{\sigma_o}{\sigma_{rr(r)}}\right)^2 - 1} - \tan^{-1}\frac{3\left(\frac{b}{\rho}\right)^2 + \eta}{\sqrt{3\eta}\left[\left(\frac{b}{\rho}\right)^2 - 1\right]}\right] \right\} \qquad (20)$$

where $\delta = 1-\nu+\nu^2$ and $\eta = (1-2\nu)^2 = 1-4\nu+4\nu^2$, and $3+\eta = 4\delta$.

TRESCA'S YIELD CRITERION

Tresca's yield criterion is based on the assumption that yielding prevails when a critically resolved shear stress is attained. In isotropic materials this is equivalent to saying that yielding prevails when the difference between the maximum principal stresses reaches a constant equal to the material's yield strength in uniaxial loading. In an internally pressurized thick-walled tube,

where the radial stress is compressive (negative) and the tangential (hoop) stress is tensile (positive), Tresca's yield criterion can be written as

$$| \sigma_{\theta\theta} - \sigma_{rr} | = \sigma_o \tag{21}$$

as long as $\sigma_{rr} \leqslant \sigma_{zz} \leqslant \sigma_{\theta\theta}$. This is certainly the case in plane-stress, and it is reasonable to assume that it prevails in plane-strain as well (however, in both cases only as long as the radial and the hoop stresses are of opposite signs).

As mentioned before, at the elastic-plastic interface, $r=\rho$, the Lamé solution and the yielding prevail simultaneously. As a result, one gets the following:

$$\sigma_{rr(\rho)} = - \frac{(\frac{b}{\rho})^2 - 1}{2(\frac{b}{\rho})^2} \cdot \sigma_o \tag{22}$$

at the elastic-plastic interface, $r=\rho$, and accordingly, the stress distribution in the elastic region, $\rho \leqslant r \leqslant b$ is

$$\sigma_{\theta\theta(r)} = \frac{(\frac{b}{r})^2 + 1}{2(\frac{b}{\rho})^2} \cdot \sigma_o \tag{23a}$$

and

$$\sigma_{rr(r)} = - \frac{(\frac{b}{r})^2 - 1}{2(\frac{b}{\rho})^2} \cdot \sigma_o \tag{23b}$$

However, with $| \sigma_{\theta\theta} - \sigma_{rr} |$ = constant = σ_o, the solution to Eq. (2) is

$$\ln \frac{r}{\rho} = \{\frac{\sigma_{rr}(r)}{\sigma_o} + \frac{(\frac{b}{\rho})^2 - 1}{2(\frac{b}{\rho})^2}\} \tag{24}$$

when Eq. (22) is applied as the boundary condition at the elastic-plastic interface, $r=\rho$. The solution to Eq. (2), when Tresca's yield criterion is assumed, is given in Eq. (24) for comparison with the equivalent solutions when Mises' yield criterion is assumed--in Eq. (11) for plane-stress and in Eq. (20) for plane-strain. Equation (24) can be rewritten, however, as

$$\sigma_{rr(r)} = \left\{ \ell n \frac{r}{\rho} - \frac{\left(\frac{b}{\rho}\right)^2 - 1}{2\left(\frac{b}{\rho}\right)^2} \right\} \cdot \sigma_o \qquad (24'a)$$

for the reader's perception of the correlation between the radius, r, and the radial stress at that surface, $\sigma_{rr(r)}$, as well as for a comparison with the tangential (hoop) stresses, $\sigma_{\theta\theta(r)}$, at the same surface within the plastically deformed region, $a \leq r \leq \rho$

$$\sigma_{\theta\theta(r)} = \left\{ \ell n \frac{r}{\rho} + \frac{\left(\frac{b}{\rho}\right)^2 + 1}{2\left(\frac{b}{\rho}\right)^2} \right\} \cdot \sigma_o \qquad (24'b)$$

AN UPPER BOUND SOLUTION

Lode (ref 6) has demonstrated that Mises' yield criterion in plane-stress deviates from Tresca's by no more than a factor of $2/\sqrt{3} \cong 1.155$. Thus, by multiplying the yield strength by $2/\sqrt{3}$ and applying it to Eqs. (22), (23a), and (23b), one can compute an upper bound solution for the radial stress at the elastic-plastic interface, $r=\rho$, and throughout the plastic region, $a \leq r \leq \rho$, respectively. By applying the higher yield strength $\left(\frac{2}{\sqrt{3}} \cdot \sigma_o\right)$ to Lamé's equations (Eqs. (1'a) and (1'b)), one gets a stress distribution in the elastic outer sleeve ($\rho \leq r \leq b$) which is uniformly greater by a factor of $\frac{2}{\sqrt{3}}$ than that

[6] W. Lode, "Versuche über den Einfluss der mittleren Hauptspannung auf das Fliessen der Metalle Eisen, Kupfer und Nickel," Z. Physik, Vol. 36, 1926, pp. 913-939.

which was obtained for Tresca's yield criterion. Indeed, if one computes the ratio between $\sigma_{rr(\rho)}$ for Mises' yield criterion in plane-stress and $\sigma_{rr(\rho)}$ for Tresca's yield criterion from Eqs. (7) and (22), respectively, one gets

$$\frac{\sigma_{rr} \text{ @ yield for Mises' yield criterion in plane-stress}}{\sigma_{rr} \text{ @ yield for Tresca's yield criterion}} = \frac{2(\frac{b}{\rho})^2}{\sqrt{3(\frac{b}{\rho})^4 + 1}} \quad (25)$$

where

$$1 \leq \frac{2(\frac{b}{\rho})^2}{\sqrt{3(\frac{b}{\rho})^4 + 1}} \leq \frac{2}{\sqrt{3}}$$

depending on the elastic wall ratio, $\frac{b}{\rho}$.

Furthermore, comparing the radial stress at the elastic-plastic interface, $r=\rho$, for Mises' yield criterion in plane-stress and in plane-strain, as expressed in Eqs. (7) and (17), respectively, suggests that $\sigma_{rr(\rho)}$ in plane-stress $\leq \sigma_{rr(\rho)}$ in plane-strain, and that

$$\lim_{\nu \to 0.5} \left\{\frac{\sigma_{rr(\rho)} \text{ for Mises' yield criterion in plane-strain}}{\sigma_{rr(\rho)} \text{ for Mises' yield criterion in plane-stress}}\right\} = \frac{2}{\sqrt{3}}$$

Thus, Tresca's yield criterion and its multiplication by $2/\sqrt{3}$ provides us with two limiting solutions--a lower and an upper bound solution--lower and higher, respectively, than those offered here for Mises' yield criterion in plane-stress and in plane-strain. However, these findings apply to the elastic region only and only while under pressure.

Comparing Eqs. (11) and (20) for the radial stress distribution in Mises' plastic zone in plane-stress and in plane-strain, respectively, with Eq. (24) for the radial stress distribution in Tresca's plastic zone, suggests that the

proportionality (between the two Mises' solutions and the two Tresca's limiting solutions) that prevails in the elastic region, $\rho \leq r \leq b$, does not necessarily prevail in the plastic region, $a \leq r \leq \rho$. This also applies to that pressure at the bore, r=a, that is computed as the one which brings about the elastic-plastic interface at $r=\rho$. The retained stress distribution after depressurization is the difference between that which is attained under load, elastic and/or plastic, minus the elastic recovery due to the removal of the applied (internal) pressure. Since the proportionality between these pressures, as computed for the two Mises' yield criteria and for the two Tresca's criteria, differs from that which prevails in the elastic region, the ratio between the corresponding retained stress distribution bears no similarity to either of them. Namely, the two Tresca solutions are not necessarily upper and lower solutions with the two Mises solutions falling between them, when comparing the retained stress distributions.

REVERSE PLASTIC DEFORMATION

The stress distribution in thick-walled tubes pressurized internally is one of radial compressive stresses and tangential (hoop) tensile stresses. If and when plastic deformation takes place in an inner sleeve, $a \leq r \leq \rho$, upon the removal of the pressure that causes such a deformation, it results in retained stress distribution whose radial component is compressive everywhere (except zero at its boundaries, r=a and r=b) and whose tangential (hoop) component varies from tensile at the tube's OD to compressive at its inner diameter (ID). In thick-walled tubes when a significant portion of the wall thickness undergoes plastic deformation upon pressurization, yielding might commence near the tube's inner wall where both the radial and the tangential components of the retained

stress are compressive. In such a case, Eqs. (4) and (14) still represent Mises' yield criterion in plane-stress and in plane-strain, respectively. However, Eq. (21) does not represent Tresca's yield criterion for reverse yielding since $\sigma_{\theta\theta}$ and σ_{rr} have the same sign. Thus, the maximum shear is normal to the r axis and is on surfaces that are 45 degrees to the x and the θ axes--and not normal to the x axis and on surfaces that are 45 degrees to the r and the θ axes, as it is upon pressurization. The suggestion that mathematically the deformation upon unloading is not the reversal of the deformation upon loading is another reason to question the applicability of Tresca's yield criterion to the process at hand, unless of course, it can be demonstrated that the value of the axial stress component is always between those of the radial and the tangential components. Tresca's yield criterion, by its own nature, ignores the third component of stress.

RESULTS

The various radial stresses for each of the above-mentioned modes of deformation at the elastic-plastic interface, $r=\rho$, were computed by using Eqs. (7), (17), and (22). With these values as the respective boundary conditions, Lamé's Eqs. (1'a) and (1'b) were applied to compute the stress distribution in the elastic region, $\rho \leq r \leq b$, and Eqs. (11), (20), and (24) were employed to compute the radial stress distribution in the plastic region, $a \leq r \leq \rho$. Equations (9), (15), and (24'b), respectively, were used in the calculation of the corresponding tangential stress distribution.

The determination of the internal pressure, $p_i = -\sigma_{rr(a)}$, that corresponds to any given elastic-plastic interface, $r=\rho$, was included in the above process. These respective values were used with the Lamé solution (Eqs. (1a) and (1b)) to

determine the stress distribution of the elastic recovery, which was then subtracted from the respective stress distributions obtained earlier for the tube under (internal) pressure. This process was repeated for several elastic-plastic interfacial radiuses at intervals of 10 percent of the tube's wall thickness.

Some of the results obtained for a tube's wall ratio of b/a = 5.00 inches/ 2.00 inches, material's yield strength σ_o = 160,000 psi, modulus of elasticity E = 30 • 10^6 psi, and Poisson's ratio ν = 0.25, are given in Figures 2 through 7. Figures 2, 3, and 4 show that there is a spread of about 15.5 percent between the stress distribution (under load) as computed by Tresca's yield criterion and by the same criterion with the yield strength being multiplied by $2/\sqrt{3}$. Furthermore, the stress distributions computed for Mises' yield criterion, both in plane-stress and in plane-strain, fall within the above-mentioned range, but with a spread of only about 4 percent between them. Figures 5, 6, and 7 display the retained stress distributions computed for the same elastic-plastic interfaces (as in Figures 2, 3, and 4, respectively), after removal of the internal pressure.

It is apparent that the relative position of the curves for the stress distributions computed for the Mises' yield criterion in plane-stress and in plane-strain, respectively, vis-à-vis the two Tresca's solutions, shifted from their relative position in the "stresses under load" curves.

Computations of the stress distribution in the "reverse plastic" region and corrections of the "retained stress distribution" accordingly, are beyond the scope of this work. Nevertheless, the approximate range of such a deformation has been computed for each of the four modes considered here and has been marked accordingly on Figure 7a.

CONCLUSIONS

Plane-strain solutions for the stress distribution during autofrettage and for the retained stresses after autofrettage have been offered here for an assumed Mises' yield criterion. Furthermore, it has been demonstrated that in conjunction with a similiar solution (ref 5) in plane-stress, Mises' yield criterion offers a narrower range than Tresca's yield criterion and its upper bound solution (when multiplied by $2/\sqrt{3}$) as two limiting conditions.

[5]R. Weigle, "Elastic-Plastic Analysis of a Cylindrical Tube," WVT-RR-6007, Watervliet Arsenal, Watervliet, NY, March 1960.

REFERENCES

1. S. Timoshenko and J. N. Goodier, Theory of Elasticity, Second Edition, Engineering Societies Monographs, 1951.
2. A. E. H. Love, A Treatise of the Mathematical Theory of Elasticity, Fourth Edition, Dover Publications, New York, 1944, pp. 102-103.
3. Betzalel Avitzur, Metal Forming: Processes and Analysis, McGraw-Hill Book Company, 1968, Chapters 4 and 5.
4. W. R. D. Manning, "The Overstrain of Tubes by Internal Pressure," Engineering, Vol. 159, 1945, pp. 101-102 and 183-184.
5. R. Weigle, "Elastic-Plastic Analysis of a Cylindrical Tube," WVT-RR-6007, Watervliet Arsenal, Watervliet, NY, March 1960.
6. W. Lode, "Versuche über den Einfluss der mittleren Hauptspannung auf das Fliessen der Metalle Eisen, Kupfer und Nickel," Z. Physik, Vol. 36, 1926, pp. 913-939.

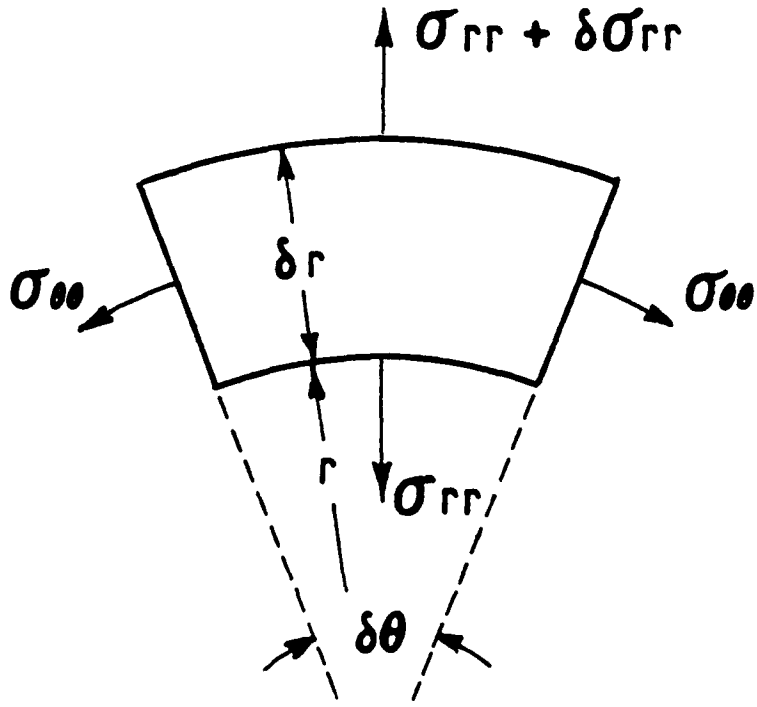

Figure 1. Stress equilibrium in a cylindrical shell.

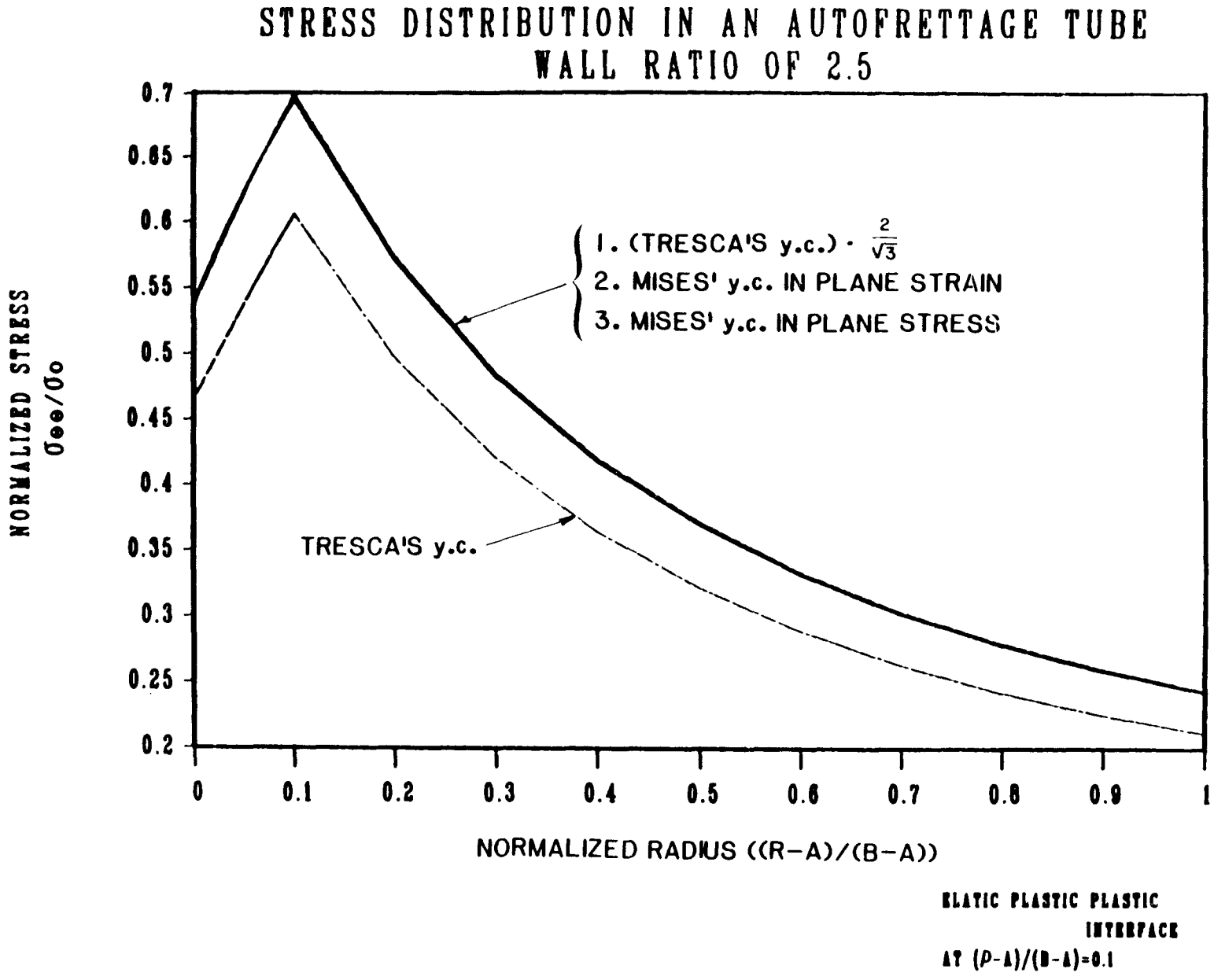

Figure 2. Stress distribution under load for 10 percent autofrettage.

(a) Tangential component of stress.

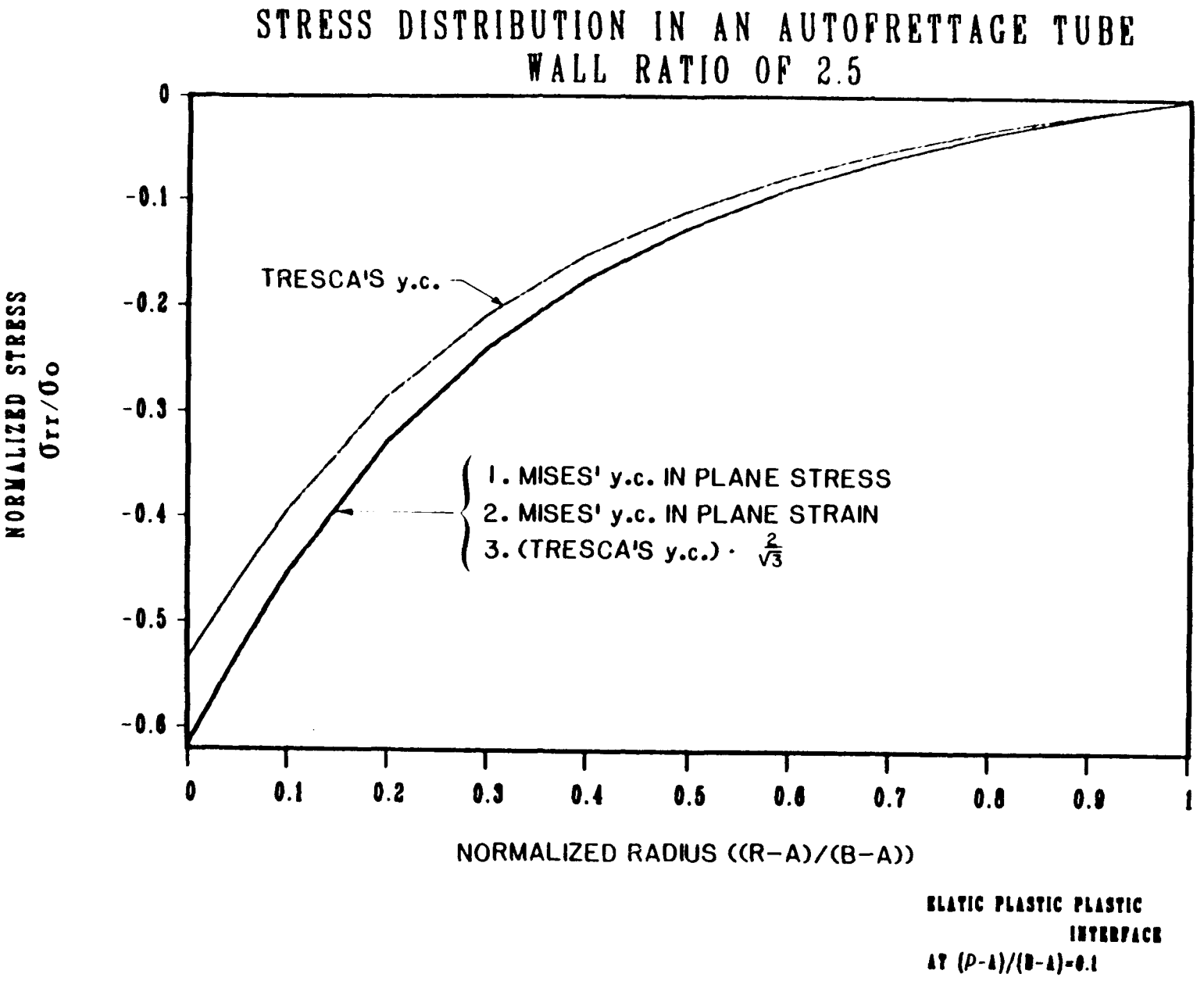

Figure 2(b). Radial component of stress.

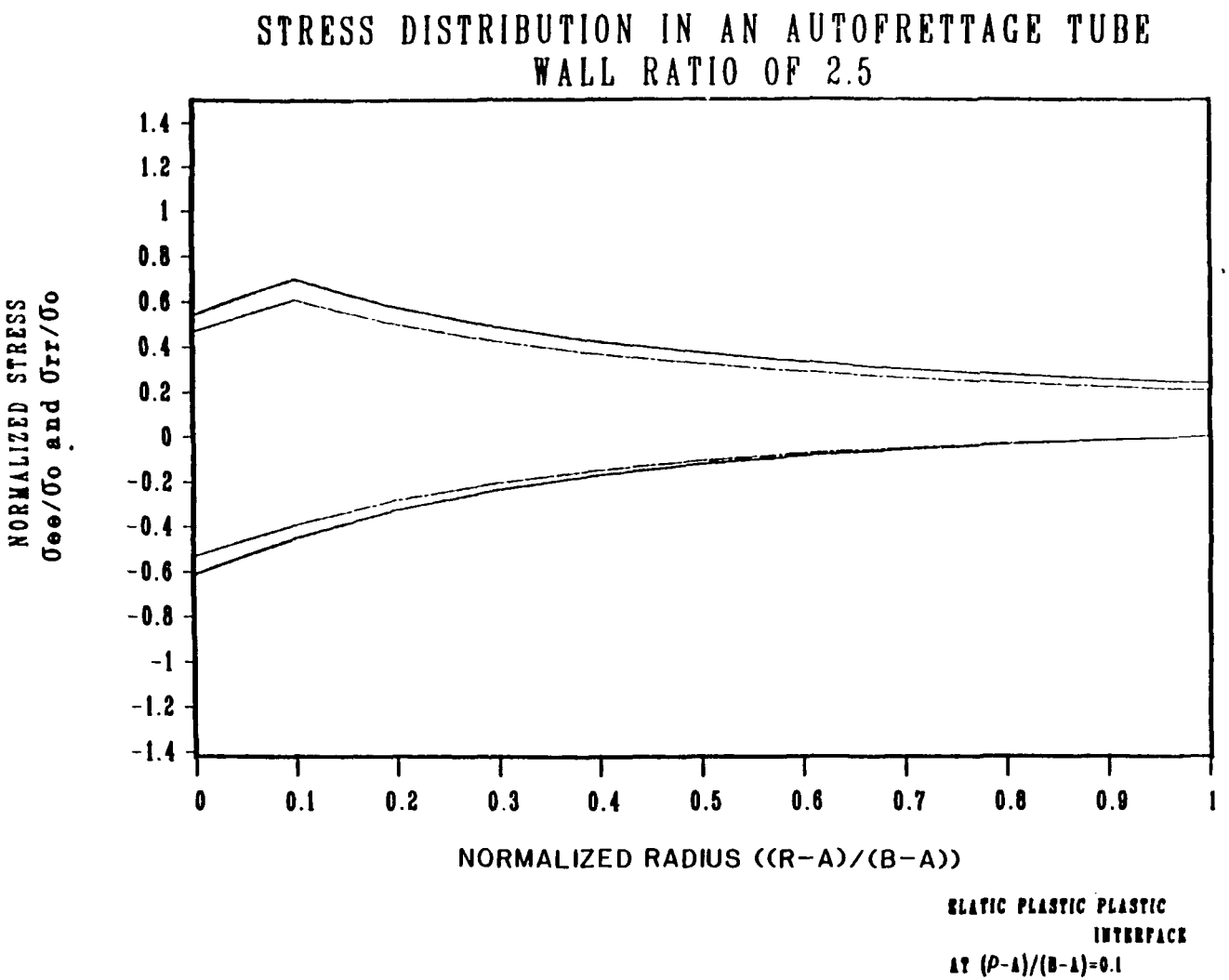

Figure 2(c). Tangential and radial components of stress (in a uniform scale).

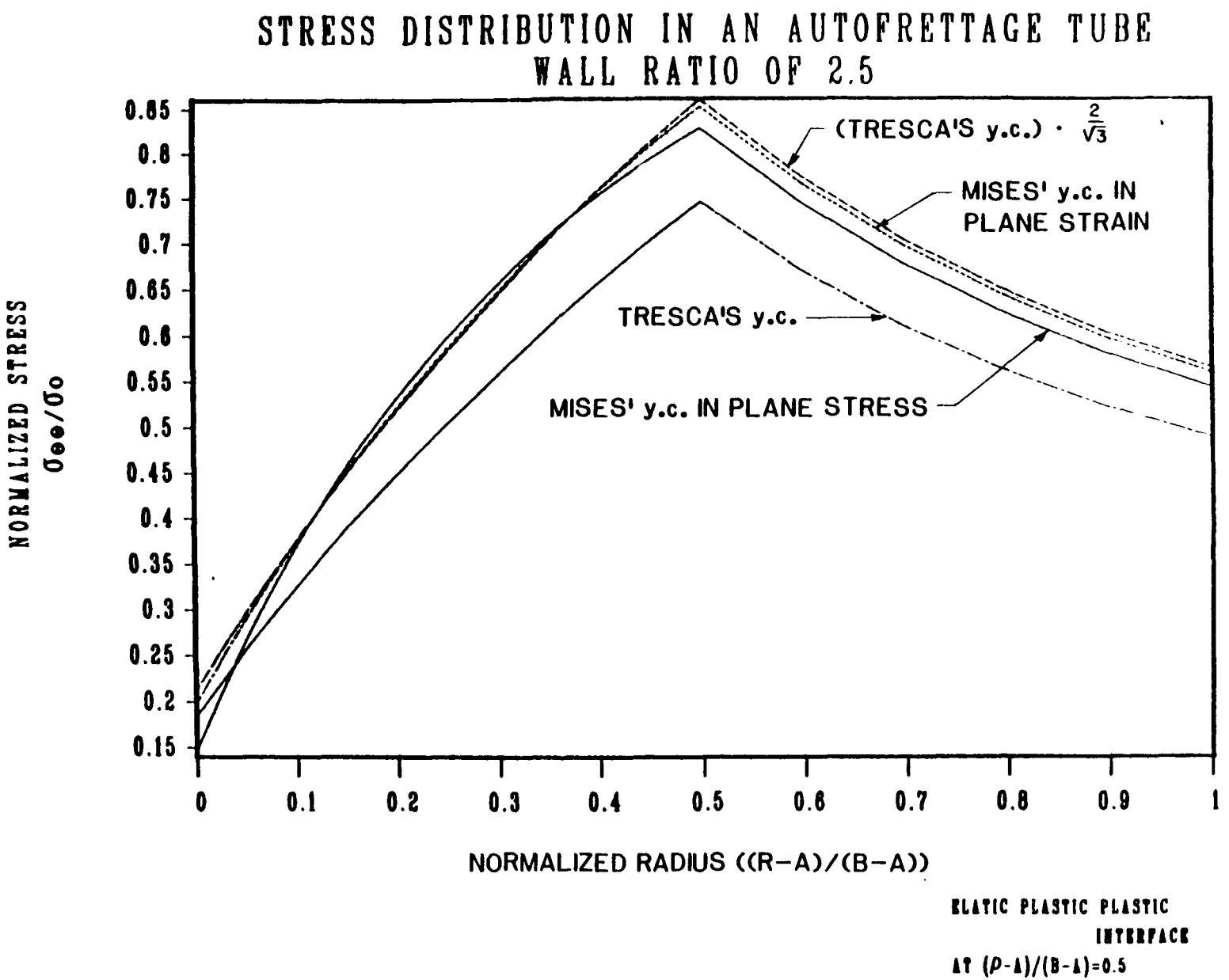

Figure 3. Stress distribution under load for 50 percent autofrettage.

(a). Tangential component of stress.

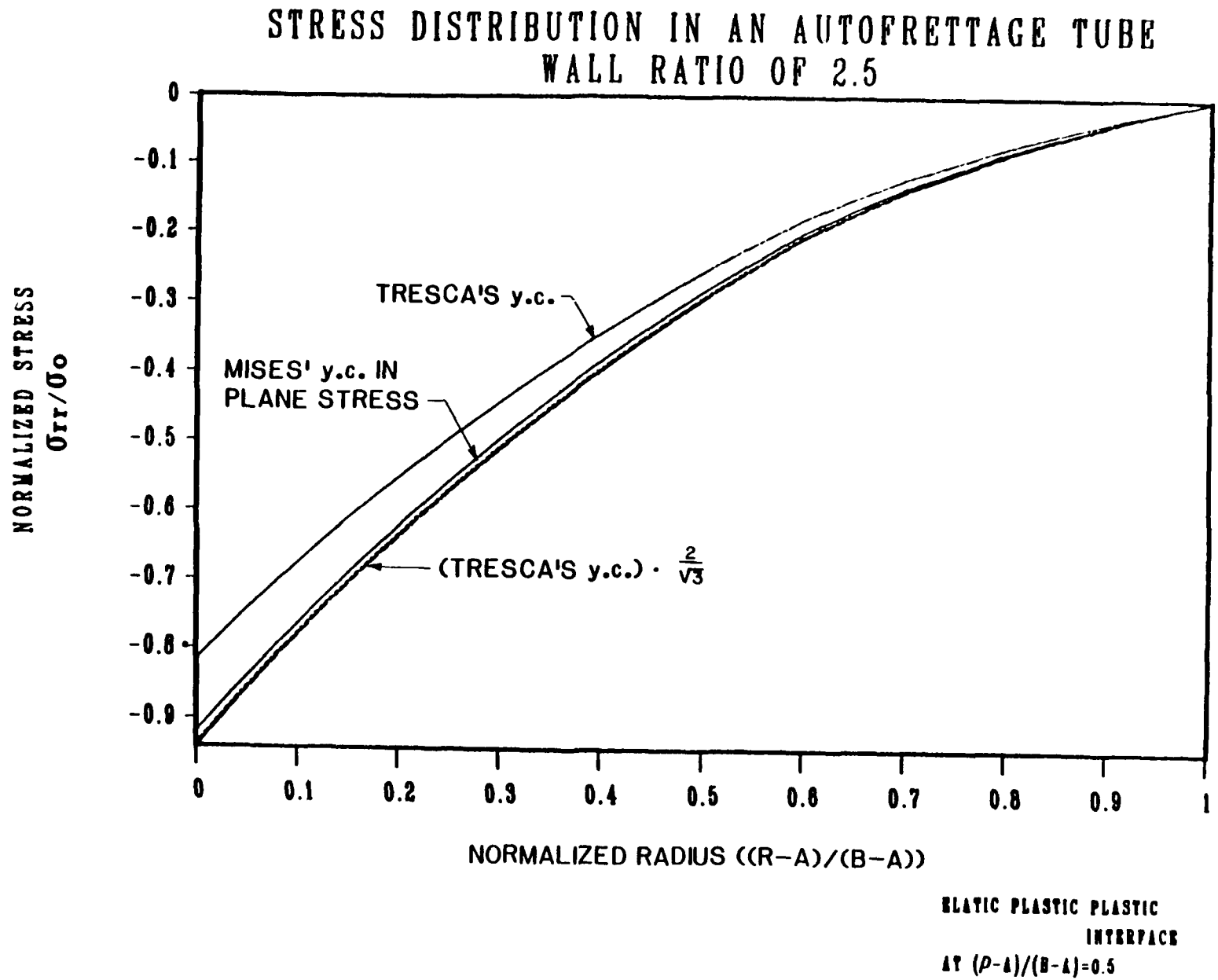

Figure 3(b). Radial component of stress.

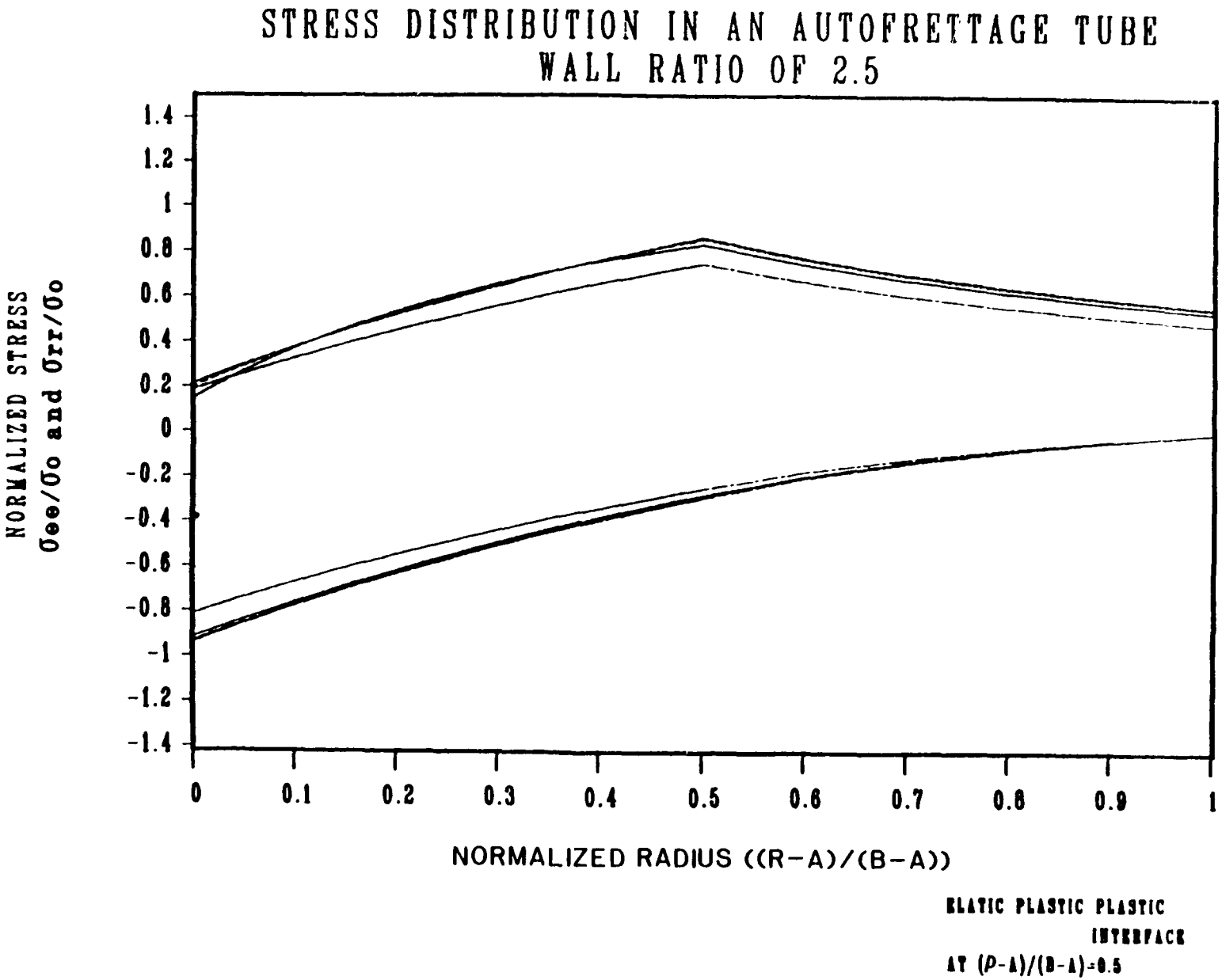

Figure 3(c). Tangential and radial components of stress (in a uniform scale).

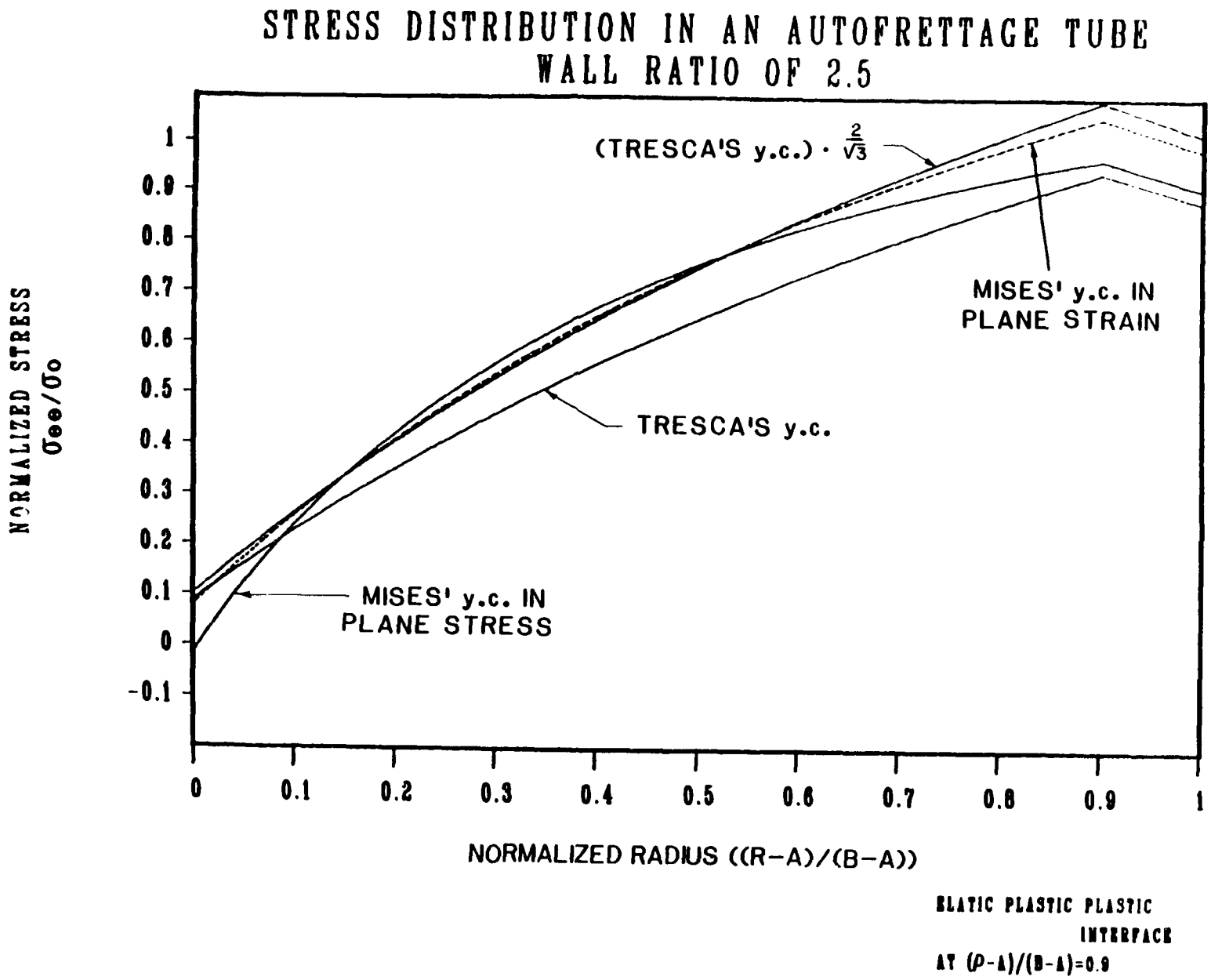

Figure 4. Stress distribution under load for 90 percent autofrettage.

(a) Tangential component of stress.

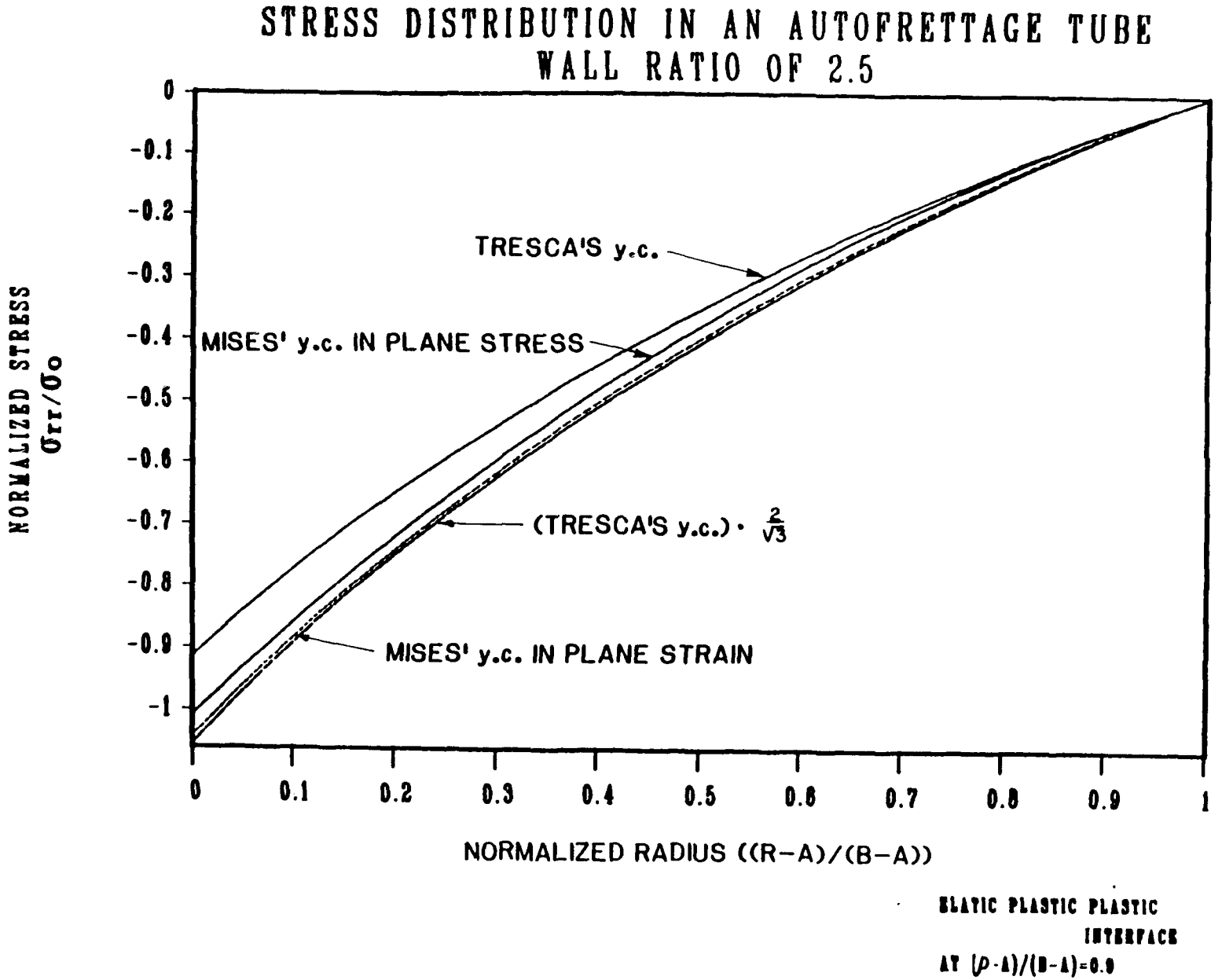

Figure 4(b). Radial component of stress.

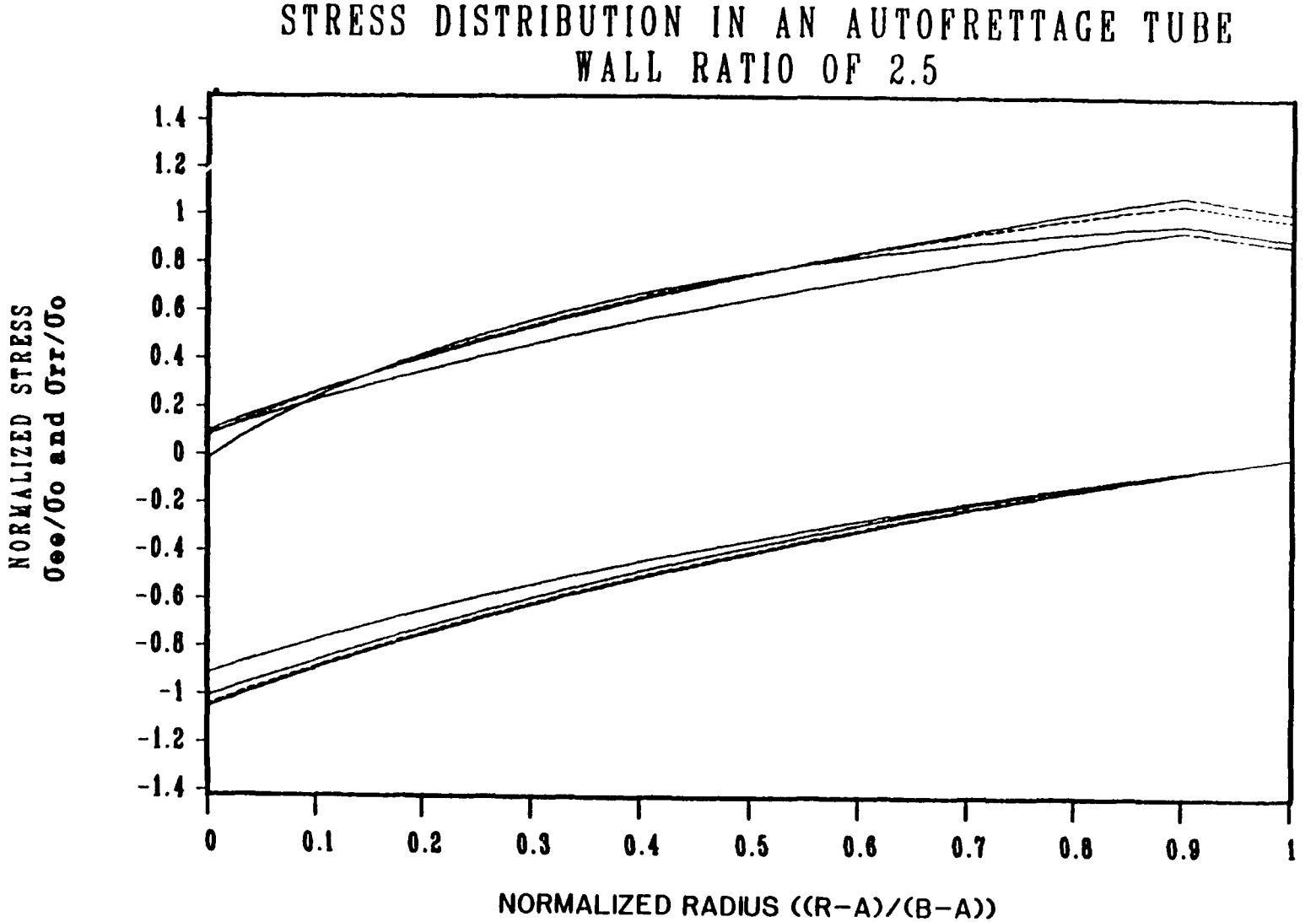

Figure 4(c). Tangential and radial components of stress (in a uniform scale).

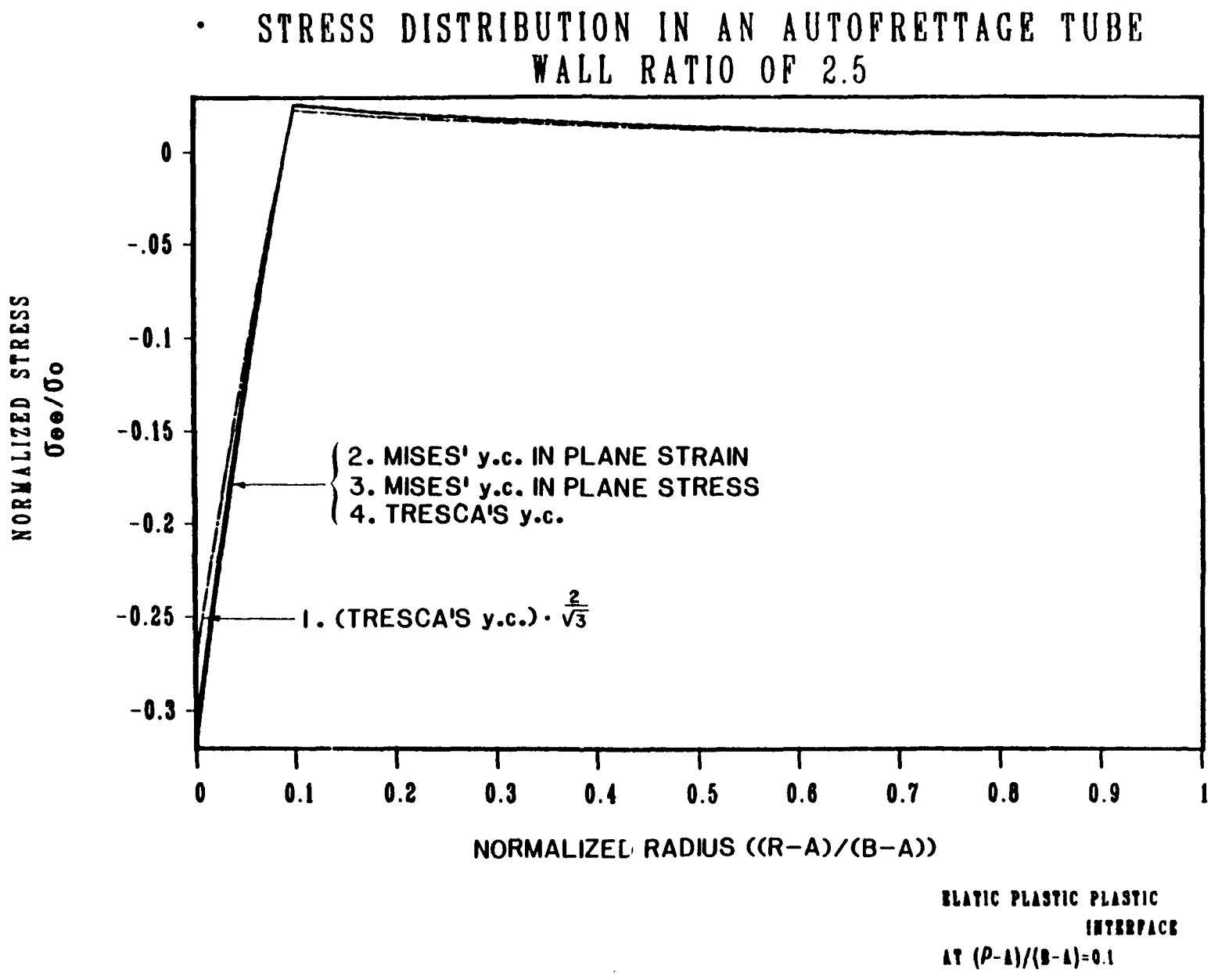

Figure 5. Retained stress distribution (after depressurization) for 10 percent autofrettage.

(a) Tangential component of stress.

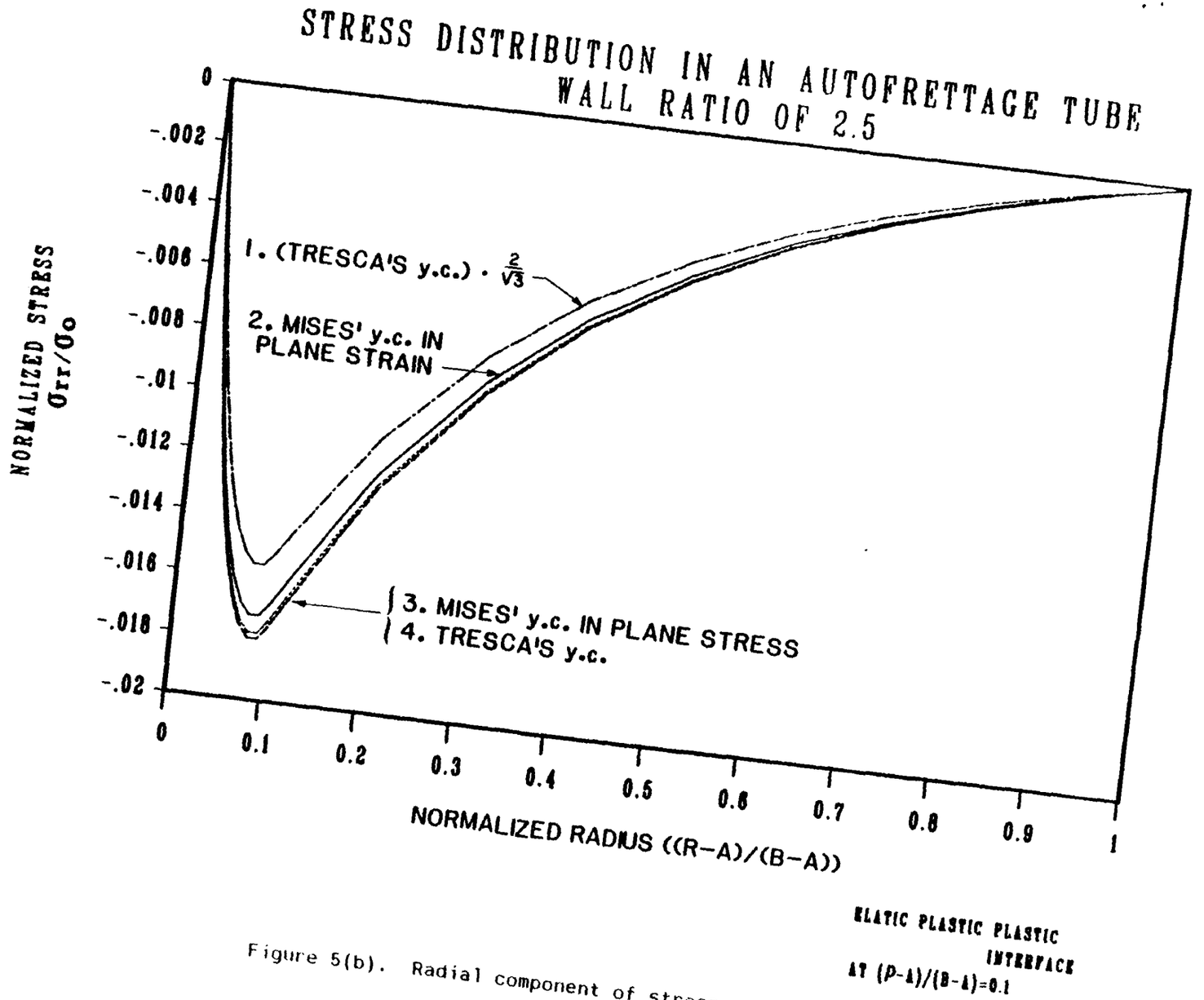

Figure 5(b). Radial component of stress.

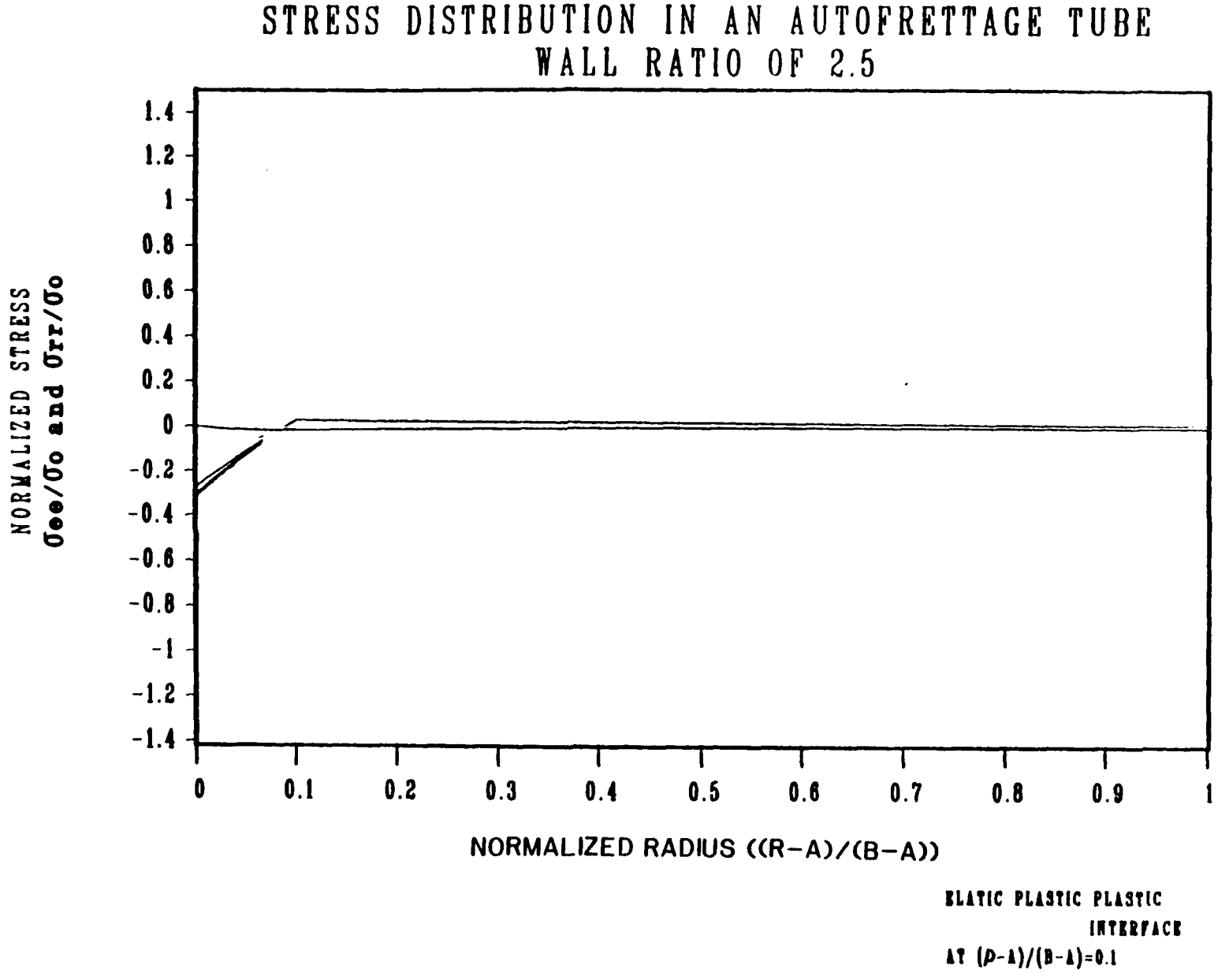

Figure 5(c). Tangential and radial components of stress (in a uniform scale).

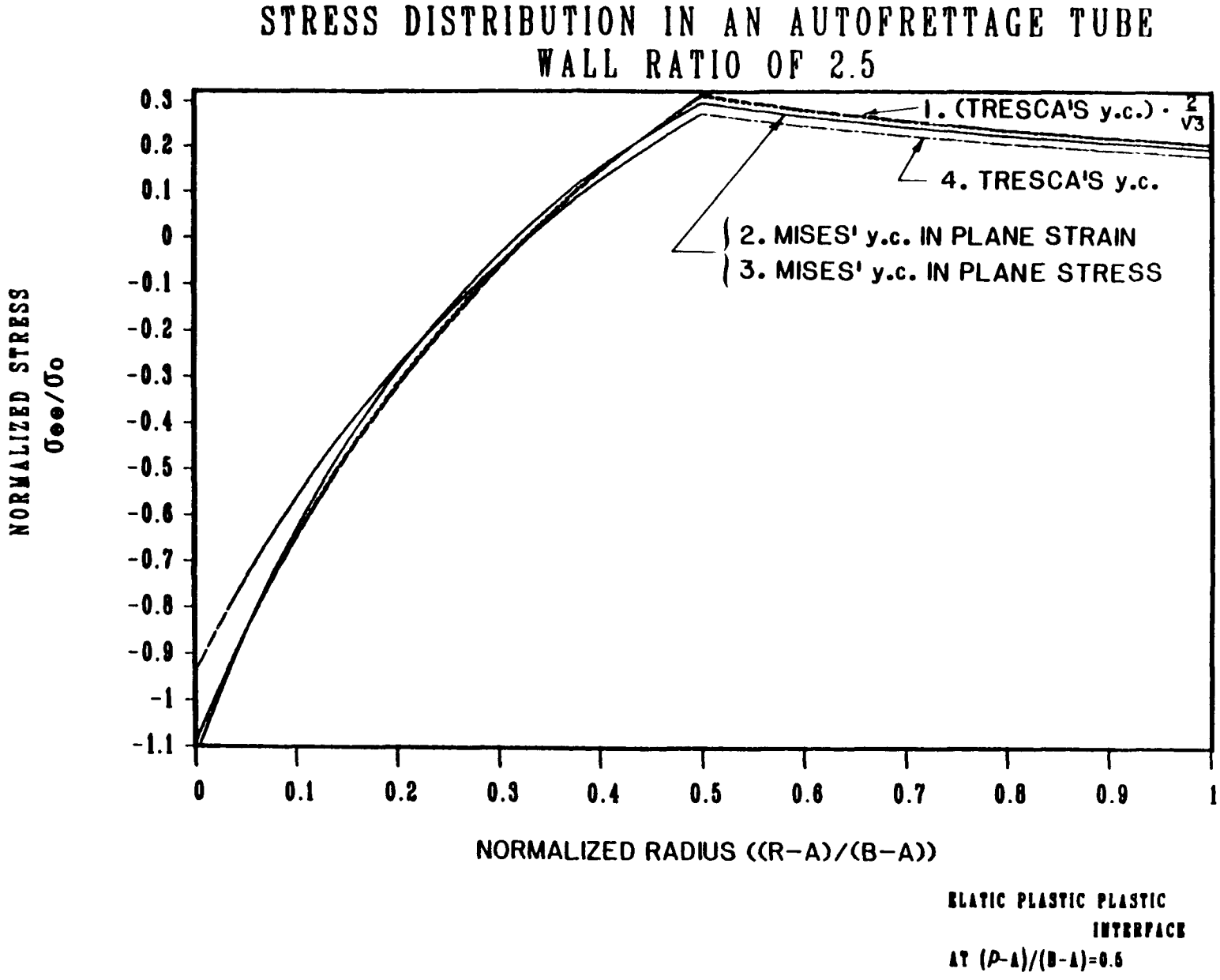

Figure 6. Retained stress distribution (after depressurization) for 50 percent autofrettage.

(a) Tangential component of stress.

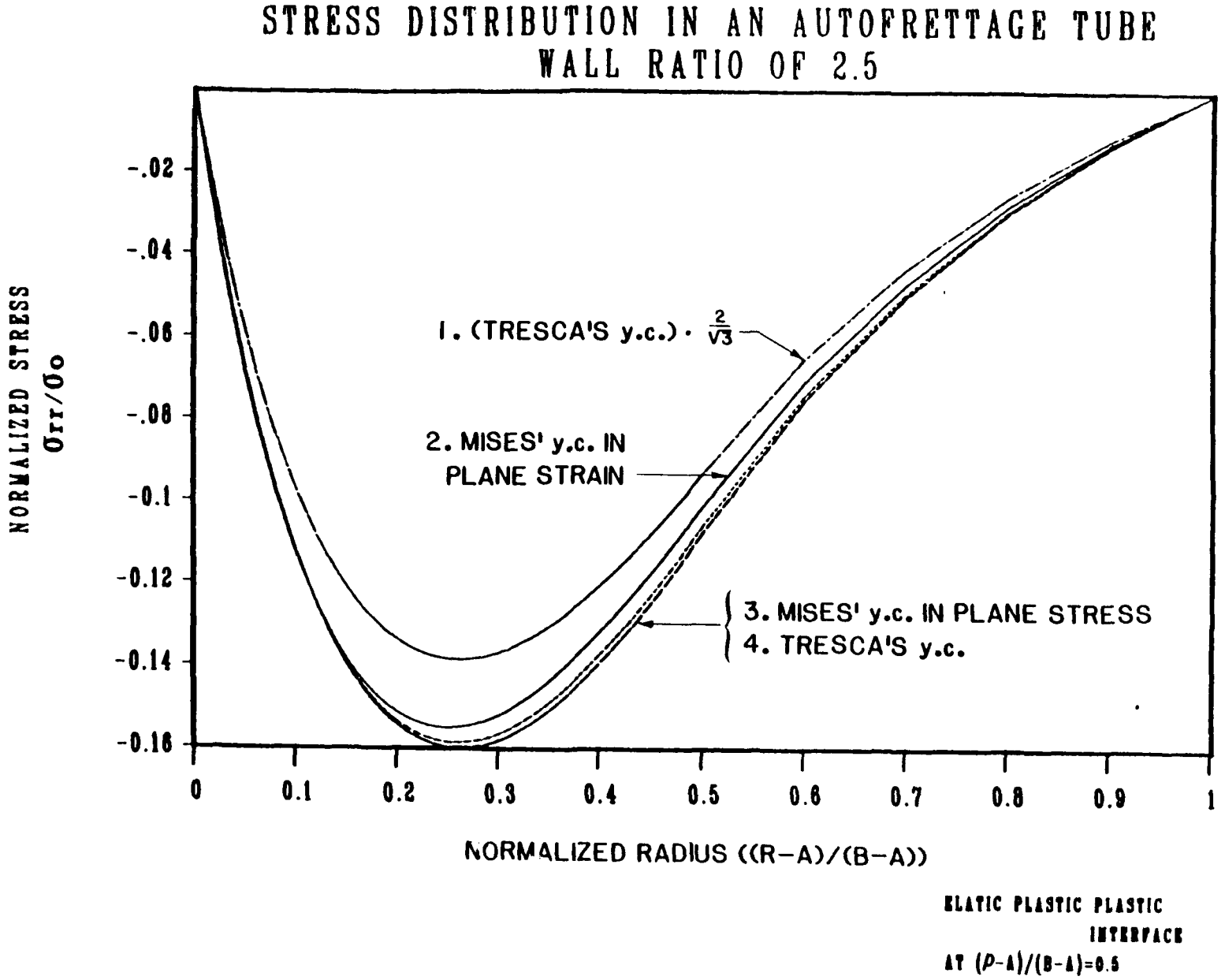

Figure 6(b). Radial component of stress.

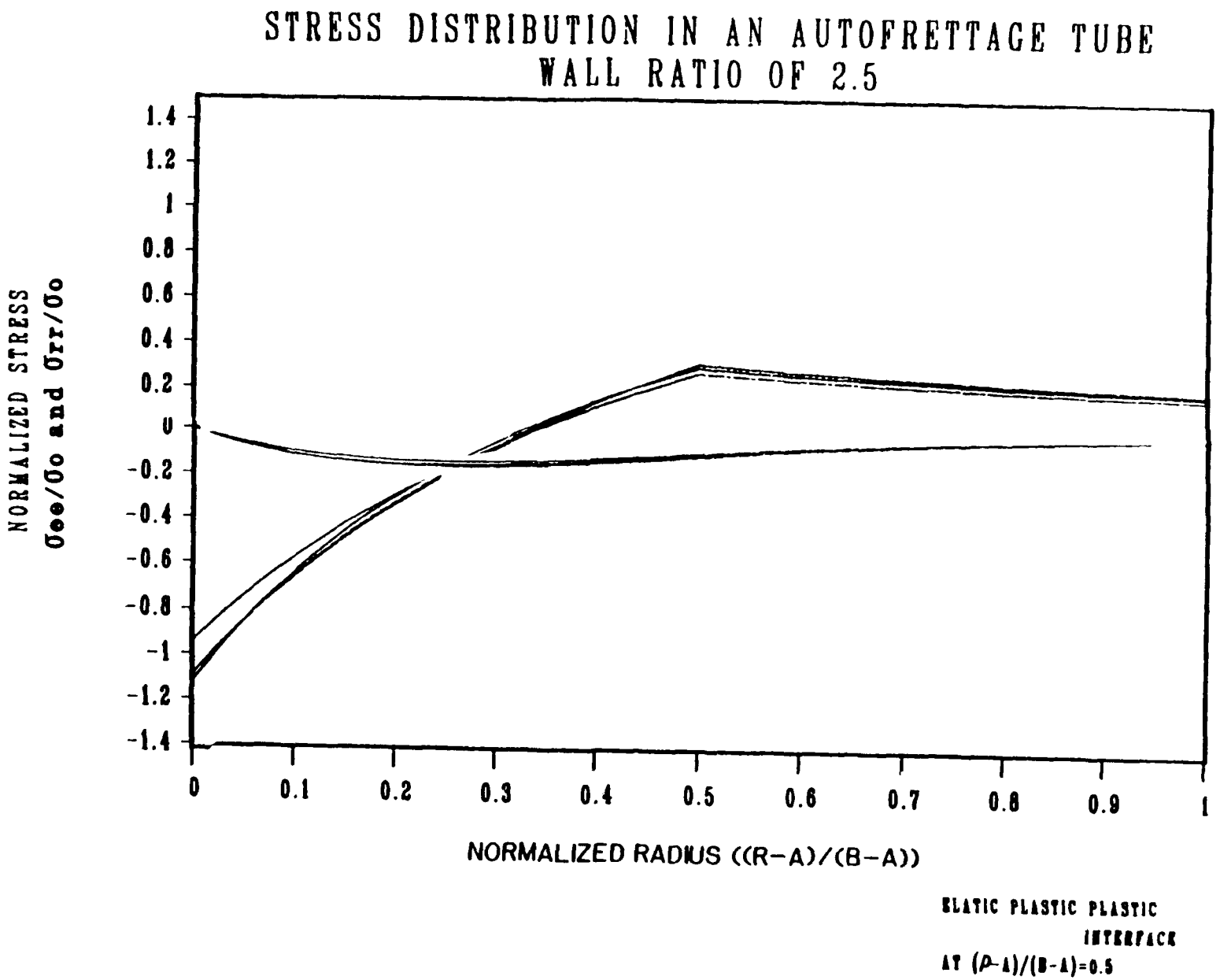

Figure 6(c). Tangential and radial components of stress (in a uniform scale).

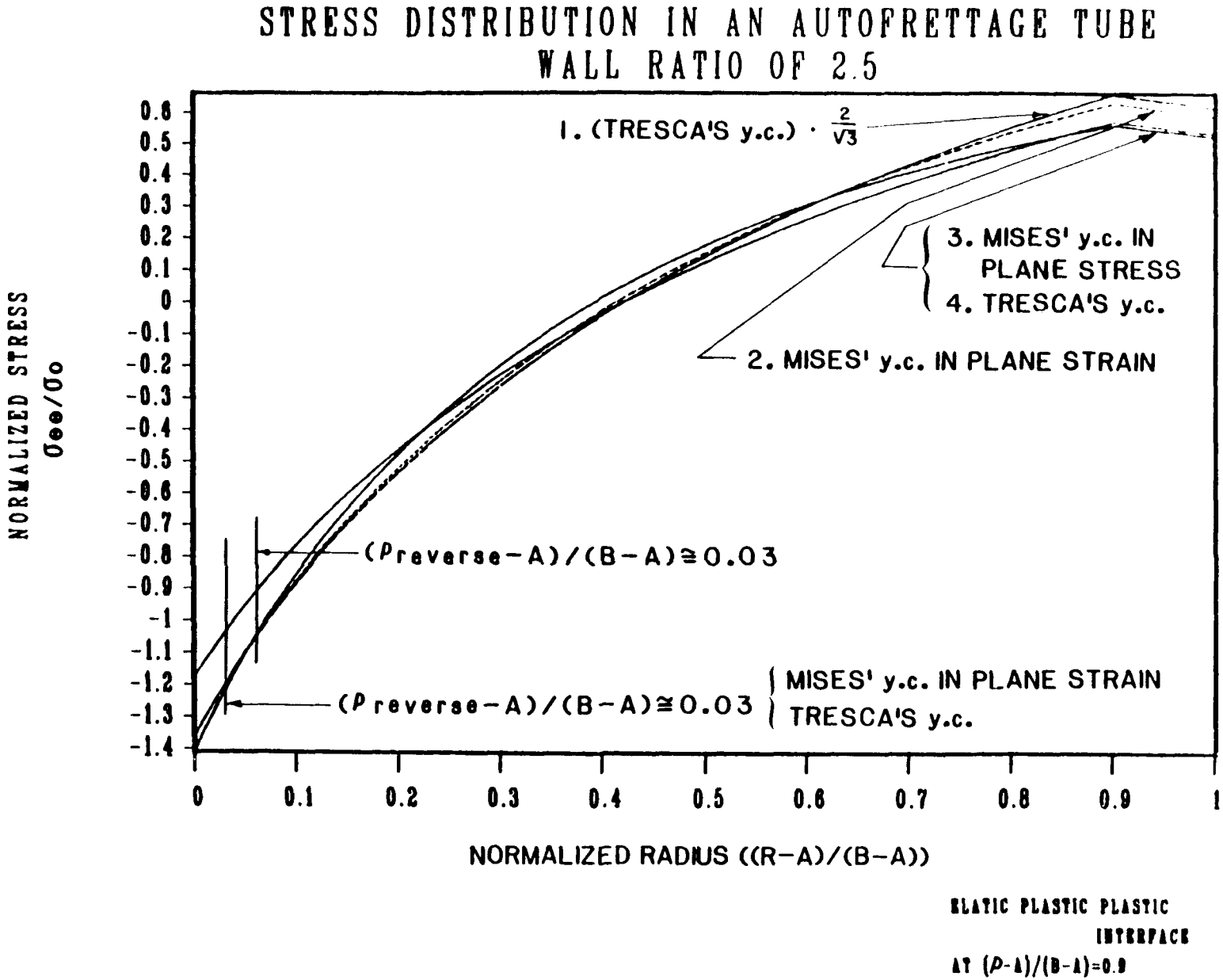

Figure 7. Retained stress distribution (after depressurization) for 90 percent autofrettage.

(a) Tangential component of stress.

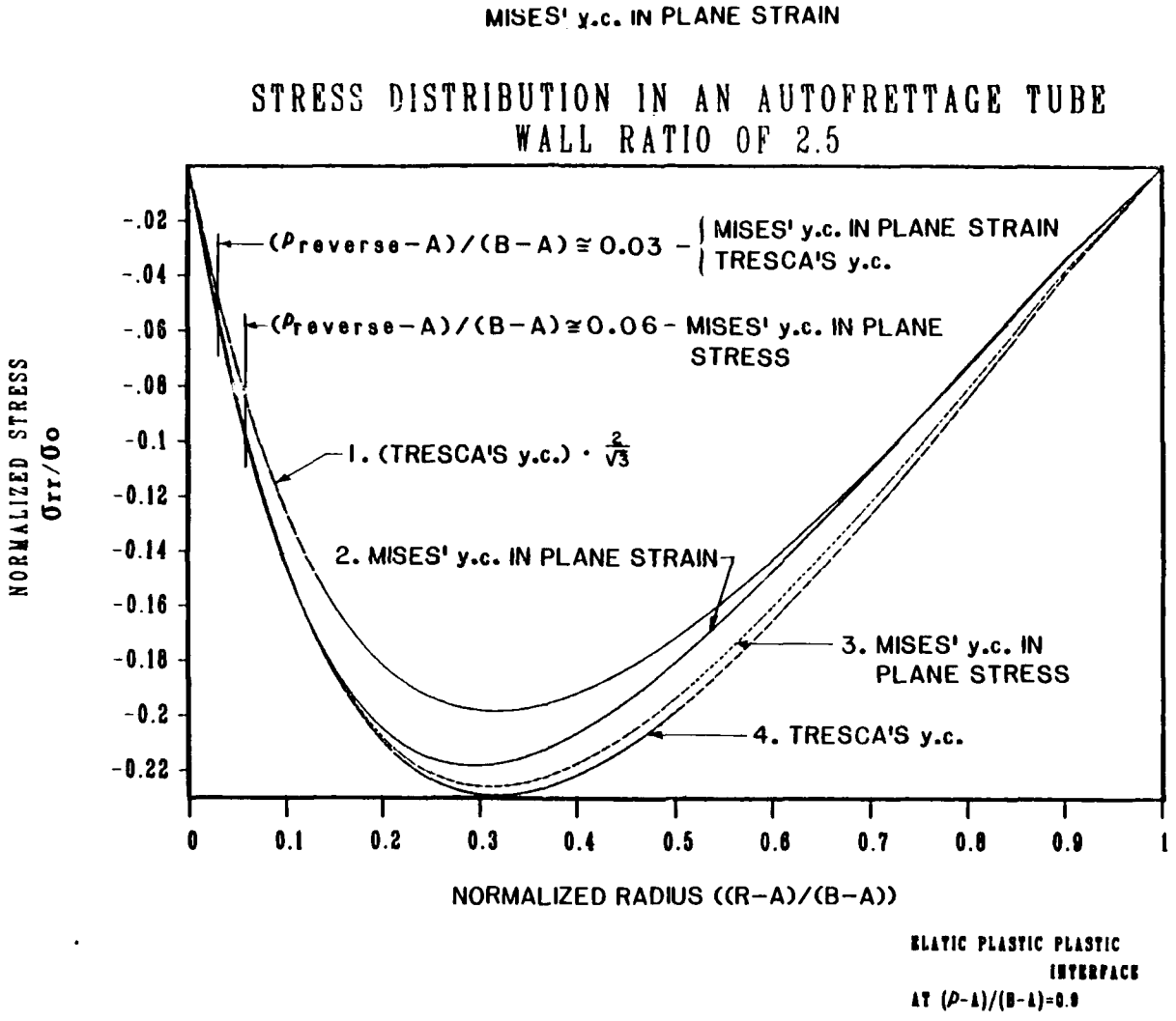

Figure 7(b). Radial component of stress.

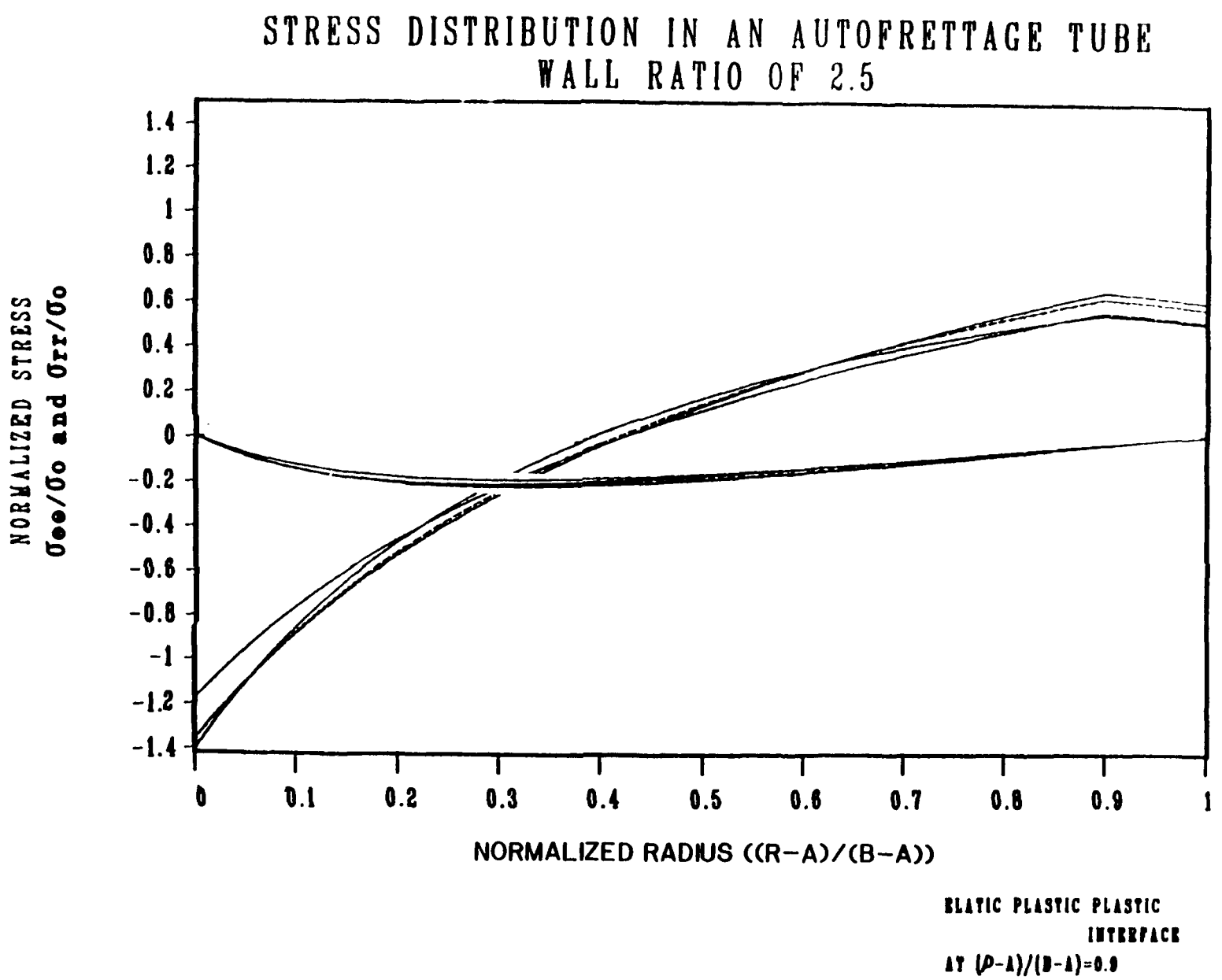

Figure 7(c). Tangential and radial components of stress (in a uniform scale).

TECHNICAL REPORT INTERNAL DISTRIBUTION LIST

	NO. OF COPIES
CHIEF, DEVELOPMENT ENGINEERING DIVISION	
ATTN: SMCAR-CCB-DA	1
-DC	1
-DI	1
-DR	1
-DS (SYSTEMS)	1
CHIEF, ENGINEERING SUPPORT DIVISION	
ATTN: SMCAR-CCB-S	1
-SD	1
-SE	1
CHIEF, RESEARCH DIVISION	
ATTN: SMCAR-CCB-R	2
-RA	1
-RE	1
-RM	1
-RP	1
-RT	1
TECHNICAL LIBRARY	5
ATTN: SMCAR-CCB-TL	
TECHNICAL PUBLICATIONS & EDITING SECTION	3
ATTN: SMCAR-CCB-TL	
OPERATIONS DIRECTORATE	1
ATTN: SMCWV-ODP-P	
DIRECTOR, PROCUREMENT DIRECTORATE	1
ATTN: SMCWV-PP	
DIRECTOR, PRODUCT ASSURANCE DIRECTORATE	1
ATTN: SMCWV-QA	

NOTE: PLEASE NOTIFY DIRECTOR, BENET LABORATORIES, ATTN: SMCAR-CCB-TL, OF ANY ADDRESS CHANGES.

TECHNICAL REPORT EXTERNAL DISTRIBUTION LIST

	NO. OF COPIES
ASST SEC OF THE ARMY RESEARCH AND DEVELOPMENT ATTN: DEPT FOR SCI AND TECH THE PENTAGON WASHINGTON, D.C. 20310-0103	1
ADMINISTRATOR DEFENSE TECHNICAL INFO CENTER ATTN: DTIC-FDAC CAMERON STATION ALEXANDRIA, VA 22304-6145	12
COMMANDER US ARMY ARDEC ATTN: SMCAR-AEE	1
SMCAR-AES, BLDG. 321	1
SMCAR-AET-O, BLDG. 351N	1
SMCAR-CC	1
SMCAR-CCP-A	1
SMCAR-FSA	1
SMCAR-FSM-E	1
SMCAR-FSS-D, BLDG. 94	1
SMCAR-IMI-I (STINFO) BLDG. 59 PICATINNY ARSENAL, NJ 07806-5000	2
DIRECTOR US ARMY BALLISTIC RESEARCH LABORATORY ATTN: SLCBR-DD-T, BLDG. 305 ABERDEEN PROVING GROUND, MD 21005-5066	1
DIRECTOR US ARMY MATERIEL SYSTEMS ANALYSIS ACTV ATTN: AMXSY-MP ABERDEEN PROVING GROUND, MD 21005-5071	1
COMMANDER HQ, AMCCOM ATTN: AMSMC-IMP-L ROCK ISLAND, IL 61299-6000	1
COMMANDER ROCK ISLAND ARSENAL ATTN: SMCRI-ENM ROCK ISLAND, IL 61299-5000	1
DIRECTOR US ARMY INDUSTRIAL BASE ENGR ACTV ATTN: AMXIB-P ROCK ISLAND, IL 61299-7260	1
COMMANDER US ARMY TANK-AUTMV R&D COMMAND ATTN: AMSTA-DDL (TECH LIB) WARREN, MI 48397-5000	1
COMMANDER US MILITARY ACADEMY ATTN: DEPARTMENT OF MECHANICS WEST POINT, NY 10996-1792	1
US ARMY MISSILE COMMAND REDSTONE SCIENTIFIC INFO CTR ATTN: DOCUMENTS SECT, BLDG. 4484 REDSTONE ARSENAL, AL 35898-5241	2
COMMANDER US ARMY FGN SCIENCE AND TECH CTR ATTN: DRXST-SD 220 7TH STREET, N.E. CHARLOTTESVILLE, VA 22901	1
COMMANDER US ARMY LABCOM MATERIALS TECHNOLOGY LAB ATTN: SLCMT-IML (TECH LIB) WATERTOWN, MA 02172-0001	2

NOTE: PLEASE NOTIFY COMMANDER, ARMAMENT RESEARCH, DEVELOPMENT, AND ENGINEERING CENTER, US ARMY AMCCOM, ATTN: BENET LABORATORIES, SMCAR-CCB-TL, WATERVLIET, NY 12189-4050, OF ANY ADDRESS CHANGES.

TECHNICAL REPORT EXTERNAL DISTRIBUTION LIST (CONT'D)

	NO. OF COPIES
COMMANDER US ARMY LABCOM, ISA ATTN: SLCIS-IM-TL 2800 POWDER MILL ROAD ADELPHI, MD 20783-1145	1
COMMANDER US ARMY RESEARCH OFFICE ATTN: CHIEF, IPO P.O. BOX 12211 RESEARCH TRIANGLE PARK, NC 27709-2211	1
DIRECTOR US NAVAL RESEARCH LAB ATTN: MATERIALS SCI & TECH DIVISION CODE 26-27 (DOC LIB) WASHINGTON, D.C. 20375	1 1
DIRECTOR US ARMY BALLISTIC RESEARCH LABORATORY ATTN: SLCBR-IB-M (DR. BRUCE BURNS) ABERDEEN PROVING GROUND, MD 21005-5066	1
COMMANDER AIR FORCE ARMAMENT LABORATORY ATTN: AFATL/MN EGLIN AFB, FL 32542-5434	1
COMMANDER AIR FORCE ARMAMENT LABORATORY ATTN: AFATL/MNF EGLIN AFB, FL 32542-5434	1
MIAC/CINDAS PURDUE UNIVERSITY 2595 YEAGER ROAD WEST LAFAYETTE, IN 47905	1

NOTE: PLEASE NOTIFY COMMANDER, ARMAMENT RESEARCH, DEVELOPMENT, AND ENGINEERING CENTER, US ARMY AMCCOM, ATTN: BENET LABORATORIES, SMCAR-CCB-TL, WATERVLIET, NY 12189-4050, OF ANY ADDRESS CHANGES.